

An Interpretation of the Vapor Phase Second Virial Coefficient Isotope Effect: Correlation of Virial Coefficient and Vapor Pressure Isotope Effects

W. Alexander Van Hook*

Chemistry Department, University of Tennessee, Knoxville, Tennessee 37996-1600

Luis Paulo N. Rebelo*

Instituto de Tecnologia Química e Biológica, UNL, Apartado 127, 2780-901 Oeiras, Portugal

Max Wolfsberg*

Chemistry Department, University of California Irvine, Irvine, California 92697-2025

Received: November 28, 2000; In Final Form: May 1, 2001

Experimental data on vapor phase second virial coefficient isotope effects (VCIEs) are reviewed and then interpreted using the general theory of isotope effects. Useful correlations are developed between $-\Delta(\mathcal{B} - b_0)/(\mathcal{B} - b_0) = (-\text{VCIE})$ and $[\ln(f_c/f_g)]^*$, where $[\ln(f_c/f_g)]^*$ is the reference condensed phase reduced isotopic partition function ratio, and \mathcal{B} is the second virial coefficient, $b_0 = 2\pi\sigma^3/3$, σ is the Lennard-Jones size parameter, and Δ denotes an isotopic difference, light-heavy. $[\ln(f_c/f_g)]^*$ can be straightforwardly obtained from measurements of vapor pressure isotope effects for $T_R = T/T_{\text{CRITICAL}} < 0.7$. We show $(-\text{VCIE}) = \ln(f_p/f_g^2)$ where $\ln(f_p/f_g^2)$ is the reduced isotopic partition function ratio associated with the equilibrium between isolated gas-phase monomer species and interacting pairs. At temperatures well removed from crossovers in $\ln(f_p/f_g^2)$ or $[\ln(f_c/f_g)]^*$, $\ln(f_p/f_g^2) = (0.4 \pm 0.2) [\ln(f_c/f_g)]^*$.

Introduction

It is well established that isotope effects (IEs) on condensed phase molar volume (MVIE), on vapor pressure (VPIE), on vapor phase virial coefficients (VCIE), and on molecular polarizability (PIE), are closely related. These isotope effects share a common origin in the vibrational properties of the molecules of interest. Van Hook and Wolfsberg¹ have shown that PIE, an effect of vibrational averaging, gives rise to an IE on the van der Waals interaction. Earlier, Wolfsberg² demonstrated that the vdW dispersion interaction includes an isotope-dependent zero point energy shift that can be expressed in terms of ground-state infrared intensities and vibrational polarizabilities. Thus the vdW dispersion interaction (and by extension more complicated interactions such as dipole–dipole, dipole–induced dipole, and hydrogen bonding) must account on one hand for the gas–gas virial coefficient interaction and the VCIE, and on the other for bulk phase condensation and the VPIE. Even so, the details of the relationships between PIE, MVIE, VCIE, and VPIE have been argued for years, sometimes contentiously.^{2–10} This situation has arisen because it has proved convenient to express virial coefficients (and VCIEs) using a parameter set that defines an intermolecular potential and IEs thereon (ϵ , σ , $\Delta\epsilon/\epsilon$, and $\Delta\sigma/\sigma$),^{3,5,11} while for the description of MVIE and VPIE it has often proved more useful to employ a formalism that uses a set of vibrational frequencies and frequency shifts, and their isotope dependences.^{12–14} Unfortunately, for VCIE, the subtleties of the vibrational averaging process that leads from a properly defined isotope independent potential function to a description of the IEs in terms of a set

of effective Lennard-Jones parameters (or parameters of some alternative intermolecular potential function) and their isotope effects, $\Delta\epsilon = \epsilon' - \epsilon = \epsilon_H - \epsilon_D$ and $\Delta\sigma = \sigma' - \sigma = \sigma_H - \sigma_D$, have not been sufficiently clearly articulated. Some confusion remains, and in the worst case, this can result in interpretations that violate the Born–Oppenheimer (BO) approximation. That BO approximation, of course, has been axiomatic in the development of the theory of equilibrium isotope chemistry.¹⁵

In the material that follows, we choose a different path to illustrate the connection between VPIE and VCIE. We compare standard state free energy differences between average condensed phase molecules or average gas-phase dimers, on one hand, and the dilute gas-phase reference on the other. The direct correlation supports the conclusion that the two effects share a common origin.

Thermodynamic Formalism. *The VPIE.* Bigeleisen has developed the thermodynamics of the vapor pressure isotope effect.^{12,16} The isotopic difference in Gibbs free energy for the condensed phases is written

$$\mu'_c - \mu_c = -RT \ln(\langle Q'_c \rangle / \langle Q_c \rangle) + (P'V'_c - PV_c) \quad (1)$$

$\langle Q_c \rangle = Q_c^{1/N}$ and $\langle Q'_c \rangle = Q'_c^{1/N}$ are properly averaged molecular partition functions, and Q'_c and Q_c are by convention the canonical partition functions for assemblies of N light (primed) and heavy (unprimed) condensed phase molecules, P' and P are equilibrium vapor pressures, and V'_c and V_c are condensed phase molar volumes not to be confused with the critical volumes V'_{crit} and V_{crit} . For the vapors, limiting corrections for nonideality to second order (i.e., through the second virial

* To whom correspondence may be addressed.

coefficient), we have

$$\mu'_g - \mu_g = -RT \ln(Q'_{g,\text{int}}/Q_{g,\text{int}}) + RT \ln(P'/P) + RT[(3/2) \ln(M'/M)] + (\mathcal{B}'_o P' - \mathcal{B}_o P) \quad (2)$$

$Q'_{g,\text{int}}$ and $Q_{g,\text{int}}$ are the canonical partition functions omitting the contribution of translation (ideal gas, denoted by the subscript g), M' and M are the molecular masses of the isotopic molecules, and \mathcal{B}'_o and \mathcal{B}_o are second virial coefficients when the vapor equation of state is written as $(PV_g/RT - 1) = \mathcal{B}_o P + 1/2 \mathcal{C}_o P^2 + \dots$. Should one choose to employ the expression $(PV_g/RT - 1) = \mathcal{B}/V_g + \mathcal{C}/V_g^2 \dots$ one finds $\mathcal{B} = \mathcal{B}_o RT$, etc. At equilibrium, $\delta\mu' = (\mu'_g - \mu'_c) = 0 = \delta\mu = (\mu_g - \mu_c)$, so $\delta\Delta\mu = (\mu'_g - \mu'_c) - (\mu_g - \mu_c) = 0$, and it follows from eqs 1 and 2 that

$$\ln(P'/P) = \ln[(Q'_{g,\text{int}} M'^{3/2} \langle Q'_c \rangle) / (Q_{g,\text{int}} M^{3/2} \langle Q_c \rangle)] + (P'V'_c - PV_c)/RT - (\mathcal{B}'_o P' - \mathcal{B}_o P)/(RT) \quad (3)$$

The first (logarithmic) term on the right-hand side, i.e., the one expressing the logarithmic ratio (condensed phase/gas phase, c/g) of isotopic partition function ratios (heavy/light, unprimed/primed) goes to zero in the classical limit (high temperature). The deviation from zero, if any, is a quantum effect. As shown originally by Bigeleisen and Mayer,¹⁶ it becomes convenient to introduce the reduced isotopic partition function ratio to express the isotopic ratio of the quantum mechanical (qm) to classical (cl) partition functions, $((s/s')f'_\beta = [(Q/Q')_{\text{qm}}/(Q/Q')_{\text{cl}}]_\beta)$, where β may be either "c" or "g", and s and s' are the symmetry numbers of the unprimed and primed molecules). Equation 4 follows directly. In eq 4 and subsequently, we suppress expression of s/s' for economy of notation and because that suppression does not affect our arguments.

$$\ln(f'_c/f_c) = \ln(P'/P) - (P'V'_c - PV_c)/RT + (\mathcal{B}'_o P' - \mathcal{B}_o P) \quad (4)$$

At low enough temperatures, i.e., not too far above the triple point, say between T_{TRIPLE} and $\sim 0.7T/T_{\text{CRITICAL}}$, the last two terms in eq 4 are small, and to good approximation one is able to employ low-temperature VPIE data to define the reference condensed phase isotopic partition function ratio, $\ln(f'_c/f_c)^*$, equal to $\text{VPIE} \sim \ln(P'/P)$.

$$\ln(f'_c/f_c)^* = \ln(P'/P) = \text{VPIE} \quad (T_{\text{TRIPLE}} < T < \sim 0.7T/T_{\text{CRITICAL}}) \quad (5)$$

In this temperature range, the vapor pressure isotope effect, $\ln(P'/P)$, is just the logarithm of the isotope effect on the equilibrium constant, $\ln(K'/K)$, corresponding to the phase change (condensed phase molecule(s) = vapor phase molecule(s))_{EQ}.^{14,17,18} Also for ($T_{\text{TRIPLE}} < T < 0.7T/T_{\text{CRITICAL}}$), the reference isotopic partition function ratio can be expressed in the form $\ln(f'_c/f_c)^* = A_c/T^2 + B_c/T$ with A_c and B_c constant. A_c contains information about the condensed phase force constants that define the external (lattice) frequencies of the molecule, and B_c contains information about the difference in the internal frequencies between the gas and the condensed phase (frequency shifts on condensation), vide infra. At higher temperatures, but below the critical temperature, one must take into account the correction factors indicated in eq 4 to calculate VPIE, and in addition the temperature dependences of A_c and B_c , if any, must be considered. The latter arise largely because the temperature dependence of the molar volume is expected to decrease A_c and

B_c when the system expands and the condensed phase structure breaks up during the approach to T_{CRITICAL} . Above T_{CRITICAL} , the reference condensed phase isotopic partition function ratio, $\ln(f'_c/f_c)^*$, has no meaning in terms of comparisons with VPIE, but its numerical value still serves as an interesting reference when considering isotopic partition function ratios of interacting pairs of gas-phase molecules in the theory of isotope effects on second virial coefficients.

An important reason for using reduced function ratios in the development that leads from eqs 1 and 2 to eqs 4 and 5 is the simple form thus obtained in the harmonic oscillator/rigid rotor approximation for the treatment of N atomic molecules. In that application $(s/s')f$ is evaluated in terms of the set of i normal mode harmonic vibrational frequencies, ν_i , $i = 1, 2, \dots, 3N$, for the condensed and vapor phases, and of the isotope effects on those frequencies. It is often useful to divide the frequencies into two classes. The first, or high-frequency class, contains harmonic modes for which $u_i = hc\nu_i/kT \sim 1.44\nu_i \text{ (cm}^{-1}\text{)}/T \gg 1$ and for which the low temperature (or zero-point energy) approximation is appropriate (see Appendix A). This class usually contains the $(3N - 6)$ nonzero frequencies of the (nonlinear) gas-phase molecule, as well as the frequencies to which they correspond in the condensed phase (i.e., the internal degrees of freedom). The second class contains the low harmonic frequencies ($u \ll 1$) which are treated in the so-called high temperature approximation (first quantum correction, Appendix A). These modes usually correspond to the six degrees of translation and rotation in the ideal gas (zero frequencies) which shift on condensation to a set of six restricted translations and rotations. These degrees of freedom are referred to as external modes. After some calculation, one obtains (Appendix A)

$$\ln(P'/P) \sim \ln(f'_c/f_c) = A_c/T^2 + B_c/T \quad (6)$$

with $A_c = (1/24)(hc/k)^2(\sum[(\nu_i^2 - \nu_i^2)_c - (\nu_i^2 - \nu_i^2)_g])$. The sum is over the low frequency (low wavenumber) set, it being understood that the six external condensed phase frequencies (three hindered translations and three hindered rotations) reduce to null frequencies in the ideal gas. Also $B_c = (1/2)(hc/k)(\sum[(\nu_i - \nu_i)_c - (\nu_i - \nu_i)_g])$; this sum is over the $(3n - 6)$ high frequencies. For linear molecules, there are but 5 external modes (3 translations, 2 rotations) and $(3n - 5)$ internal modes; for monatomics there are only 3 external modes (all translations) and no internal modes. For more rigorous analysis, instead of using eq 6, one evaluates $\ln(f'_c/f_c)$ with complete expressions for condensed and vapor phase partition functions, sometimes including corrections for nonclassical gas-phase rotation and/or vibrational anharmonicity (Appendix A). Those refinements notwithstanding, it is true that eq 6 accurately expresses the basic physical chemistry of the VPIE and may be usefully employed for the empirical representation and (sometimes) for extrapolation of VPIE data to higher or lower temperature. [For instance, for CH_4/CD_4 and $\text{CH}_4/\text{CH}_3\text{D}$, it was shown^{19,20} that an extrapolation of low-temperature VPIE data using two parameters (eq 6) could represent new data^{3,21} in the critical region (~ 60 K higher) to 0.1%.] A similar conclusion can be inferred from data for $^{36}\text{Ar}/^{40}\text{Ar}$. Here, new high precision VPIE data²² nicely described using the two-parameter fit (eq 6), are found to be in excellent agreement with older data²³ at higher (as much as 45 K) or lower (as much as 20 K) temperature when extrapolated using the two-parameter fit.²² Thus, the form of eq 6 suffices for an adequate, albeit empirical, representation of lattice anharmonicity over the liquid range.²⁰ This is an important point in the discussion that follows, since experimental

data for both VPIE and VCIE are not usually available for the same temperature range. A more complete discussion of the relationships between $\ln(f_c/f_g)^*$, $\ln(f_c/f_g)$, their representations using pseudoharmonic and harmonic models, and $\ln(P'/P) = \text{VPIE}$, as T increases toward the critical region where molar volume and vapor nonideality corrections become important, and eventually dominate, is given in Appendix B. Appendix B makes it clear that the comparison of interest to us in this paper is that between the properties of the ideal gas-phase dimers with those of the low-temperature liquid-phase not too far from its triple point, i.e., with $\ln(f_c/f_g)^*$.

The VCIE. The theory of the second virial coefficient of gases is well understood.^{11,24,25} In classical statistical mechanics, one obtains for the virial coefficient of a monatomic gas

$$\mathcal{B} = -2\pi N_A \int [\exp(-\phi_{(2)}(r)/kT) - \exp(-\phi_{(1)}(r)/kT)] r^2 dr \quad (7)$$

where $\phi_{(2)}(r)$ is the potential of interaction between two atoms, $\phi_{(1)}(r)$ is the one atom potential function (i.e., $\exp(-\phi_{(1)}(r)/kT = 1$), and N_A is Avogadro's number. The coordinate r is the distance between the two atoms. Using a statistical argument, Rice²⁵ has shown that it is reasonable to replace eq 7 with eq 8.

$$\mathcal{B} = (2/3)\pi\sigma^3 - K(T) \quad (8)$$

In eq 8, $2K(T)$ is the integrated excess probability of finding two atoms in the gas closer to each other than they would be in a random distribution with no two atom potential. This probability has been set equal to the value of the equilibrium constant K for the dimer association of the monatomic gas (the factor of 2 arises because two atoms form one dimer molecule). K here refers to the equilibrium constant expressed in terms of molecular densities of dimer and monomer, respectively, and has units of volume. The first term, $(2/3)\pi\sigma^3$ (referred to here and elsewhere as b_o), arises from the fact that the two body potential $\phi_{(2)}(r)$ has a long-range attractive portion but at short range (distances less than σ) is strongly repulsive. At short range ($r < \sigma$), the first term in the integral in eq 7 rapidly goes to zero, while the second term is equal to unity for the monatomic virial coefficient. Thus, $(2/3)\pi\sigma^3$ is the volume excluded by the short-range repulsion. For large r , when $\phi_{(2)}(r)$ goes to zero, the integral in eq 7 also goes to zero. At intermediate values of r , the integrand is positive because $\phi_{(2)}(r)$ is a binding potential. Equation 8 correctly explains the temperature dependence of observed virial coefficients—positive values at high T where K approaches zero, decreasing positive values as temperature decreases, becoming negative as T continues to decrease depending on the strength of the two body interaction $\phi_{(2)}(r)$.

It is noteworthy that one can obtain the relationship between \mathcal{B} and the equilibrium constant K by considering a thermodynamic equilibrium between stable dimer A_2 and monomer A species ($2A = A_2$), then assuming both A and A_2 to be ideal gases, and finally calculating the total pressure of the system. This line of thermodynamic reasoning yields $\mathcal{B} = -K$. The equilibrium constant K is a positive quantity, approaching zero at high temperature. One also knows that the hard sphere second virial coefficient of a gas is b_o and that, indeed, second virial coefficients tend to be positive at higher temperatures. Thus, one can reason that eq 8 is a reasonable representation of \mathcal{B} .

For calculation of virial coefficients of polyatomic molecules, the theoretical formulation in classical statistical mechanics becomes more complicated than eq 8 since many molecular degrees of freedom need to be considered. However, what

remains, the same as eq 8, is that one still calculates the difference between an integrated probability for finding two molecules close to each other when the two molecule interaction is included and the probability of finding the two molecules at the same distance in the absence of the two molecule interaction. One is led to an equation for the virial coefficient of the same form as that given in eq 8 with the two terms again being an excluded volume and an association equilibrium constant. With eq 8, there is no isotope effect on the second virial coefficient in classical mechanics. The first term in eq 8 depends only on the potential parameter σ which is independent of isotopic substitution in the BO approximation, and it is well-known in isotope chemistry that an equilibrium constant formulated using classical statistical mechanics, K_{cl} , is independent of isotopic substitution.¹⁶

In making the transition to quantum statistics, we note that it has been shown²⁴ that quantum statistical mechanics yields an expression similar to eq 7 for the second virial coefficient of a monatomic gas. It is only necessary to replace the Boltzmann factors, $\exp(-\phi_{(i)}(r)/kT)$, by the corresponding normalized Slater sums (the normalizing factor has been omitted in eq 9)

$$\sum \psi_n^*(r) [\exp(-(\mathbf{T} + \phi_i)/kT)] \psi_n(r) \quad (9)$$

where the $\psi_n(r)$'s correspond to an appropriate orthonormalized complete set of functions and the summation is over this complete set. \mathbf{T} is the quantum mechanical operator for kinetic energy and the functions $\phi_i(r)$ correspond to $\phi_1(r)$ or $\phi_2(r)$ of eq 7. The important point to recognize is, for $r < \sigma$, the potential remains strongly repulsive so that the contribution to \mathcal{B} only arises from the second term in eq 7 (quantum version) and the excluded volume, $(2/3)\pi\sigma^3$ is again obtained. Similarly, the two terms in the quantum mechanical equivalent of eq 7 cancel at large values of r where the two atom interaction disappears. Thus, we are led again to eq 8 for the virial coefficient except that now K is to be formulated quantum mechanically. Note that the quantum mechanical equilibrium constant K is isotope dependent. The statistical mechanical formulation of the equilibrium constant for pair formation should be written as the ratio of the partition function for two monomers in the presence of the interaction potential between monomeric species (and including the appropriate summation of continuum states above the dissociation limit) and the corresponding partition function for two monomers in the absence of an interaction potential.^{11,26} In our model, we consider K in the "harmonic approximation", replacing it by a bound dimer (pair) harmonic-rigid-rotor partition function divided by the square of the harmonic partition function of the corresponding monomer, $\ln(f_p/f_g^2)$.

Since $b_o = (2/3)\pi\sigma^3$ is isotope independent, one focuses the discussion of VCIE in the context of eqs 8 and 9 on $(\mathcal{B} - b_o)$, which is directly related to the association equilibrium constant K . Continuing, we develop expressions for $(-\text{VCIE}) = \ln(f_p/f_g^2)$ analogous to those for $\ln(f_c/f_g)^*$ by recalling that the vapor pressure may be regarded as the equilibrium constant for the reaction (liquid = vapor). Consequently, because the reduced partition function ratio (f_c/f_g) refers to isotopic ratios of partition functions in the condensed and vapor phases, one expresses $\ln(P'/P)$, by relating it to (f_c/f_g) and $(f_c/f_g)^*$, see eq 5. In the present communication, we establish the relationship by comparing $(f_c/f_g)^*$ values obtained from VPIE to corresponding (f_p/f_g^2) values obtained from VCIE. The isotope effect on the association equilibrium constant K is expressed in terms of reduced partition function ratios as $\ln(K'/K) = \ln(f_g^2/f_p)$ in precise analogy to eq 5. We define VCIE as follows.

$$\ln(K/K') = -\ln(K'/K) = \ln(f_p/f_g^2) = -\ln[(\mathcal{B} - b_o)'/(\mathcal{B} - b_o)] = (-\text{VCIE}) = A_p/T^2 + B_p/T \quad (10)$$

The reason for the minus sign clearly rests on the fact that K involves the equilibrium (2-monomer = pair) but the vapor pressure equilibrium involves (condensed phase = monomer). Equation 10 defines VCIE and establishes its relationship to the measured values of the virial coefficient and to the A_p and B_p parameters. Also $b_o = (2/3)\pi\sigma^3$ is the excluded volume per particle, and σ is the size parameter in the Lennard-Jones, Sutherland, or other intermolecular potential; b_o values have been tabulated for some common molecules.¹¹

Further discussion of eq 10 is appropriate. When considering isotope effects on any property that can be described in terms of partition functions, including virial coefficients, it is customary to focus on quantum mechanical corrections to ratios of classically formulated partition functions, recognizing that at high enough temperature the correct quantum mechanical formulation must approach the classical limit. For the second virial coefficient, $\lim(T \rightarrow \infty)[\mathcal{B}] = b_o$, which implies $b_o = b'_o$ since $\lim(T \rightarrow \infty)[\mathcal{B}/\mathcal{B}'] = b_o/b'_o = 1$. Indeed, b_o depends only on the potential function which is isotope independent. As T falls below its high-temperature limit, \mathcal{B} drops off from the small positive value, b_o , characterizing the excluded volume contribution, through zero, to much larger negative values which are a consequence of the attractive part of the intermolecular potential. Further, using $\Delta\mathcal{B} = \mathcal{B}' - \mathcal{B}$ and recognizing that $\Delta\mathcal{B}/(\mathcal{B} - b_o) \ll 1$ and $\Delta b_o = b'_o - b_o = 0$, we obtain

$$\ln(f_p/f_g^2) = (-\text{VCIE}) = -\ln[(\mathcal{B} - b_o)'/(\mathcal{B} - b_o)] = -\ln[1 + \Delta\mathcal{B}/(\mathcal{B} - b_o)] = -\Delta\mathcal{B}/(\mathcal{B} - b_o) \quad (11)$$

As already noted, in applying the harmonic model to VCIE (eq 10), the partition functions of pair and monomer are normally written in the rigid rotor-harmonic oscillator approximation. As in the treatment of the vapor pressure isotope effect, the factor A_p in the next but last term on the right contains a sum over the low frequencies in the dimer, that is a sum over those frequencies of the interacting pair that correlate with the zero frequency monomer translations/rotations. The B_p factor (in the last term on the right of eq 10), on the other hand, treats the higher frequency internal vibrations that are expected to have shifted slightly during the transition from the ideal gas monomers to the interacting pair. One then obtains by analogy to A_c and B_c of eq 6, $A_p = (1/24)(hc/k)^2(\sum [(v_i'^2 - v_i^2)_d - (v_i'^2 - v_i^2)_g])$ and $B_p = (1/2)(hc/k)(\sum [(v_i' - v_i)_d - (v_i' - v_i)_g])$, see Appendix A. The sum in the expression for A_p for a nonlinear polyatomic molecule extends over the 12 frequencies corresponding to the so-called external degrees of freedom, which in the monomers are the rotations and translations of the two molecules (and which have zero frequencies in the monomers); in the dimer those 12 frequencies correspond to the three rotations and three translations of the dimer molecule (which again are zero frequencies), plus six frequencies that correspond first to one monomer–monomer stretch (denoted here by the subscript LJ), and five other low lying frequencies that we describe as loose monomer–monomer bending modes or hindered internal rotations. The remaining $2(3n - 6)$ internal frequencies of the two n -atomic monomers map into the same number of internal frequencies of the dimer, slightly shifted in frequency from the monomer frequency; the summation over these larger frequencies (referred to as internal frequencies) appears in the B_p term. Incorporating these considerations into eq 10, we obtain eq 12a.

$$\ln(f_p/f_g^2) = (-\text{VCIE}) = A_p/T^2 + B_p/T = (1/24)(hc/kT)^2 \left\{ \sum_{2(3n-6)}^5 [(v_i'^2 - v_i^2)_{\text{Bend,Int. Rot}}] + (v_i'^2 - v_i^2)_{\text{LJ}} \right\} + (1/2)(hc/kT) \left(\sum [(v_i' - v_i)_p - (v_i' - v_i)_g] \right)_{\text{INT}} \quad (12a)$$

The analogous equation for $\ln(f_c/f_g)^*$ is obtained from eqs 5 and 6,

$$\ln(f_c/f_g)^* = A_c/T^2 + B_c/T = (1/24)(hc/kT)^2 \left\{ \sum_{(3n-6)}^6 [(v_i'^2 - v_i^2)_{\text{EXT.lattice modes}}]_c + (1/2)(hc/kT) \left(\sum [(v_i' - v_i)_c - (v_i' - v_i)_g] \right)_{\text{INT}} \right\} \quad (12b)$$

The first sum on the right-hand side of eq 12b is over the six external lattice modes of the condensed phase molecule (corresponding once again to zero frequency gas-phase translations and rotations), and the second treats the $(3n - 6)$ remaining “internal” frequencies in condensed (subscript c), and gas phase (subscript g). Equations 10, 11, and 12a are consistent with the earlier thermodynamic analysis of Phillips, Linderstrom-Lang, and Bigeleisen.²⁷

Study of eqs 12a and 12b reveals that A_p and A_c are inherently positive. This results because $(v_i'^2 \geq v_i^2)_p$ and $(v_i'^2 \geq v_i^2)_c$ (recall the prime refers to the more lightly substituted molecule), and $(v_{\text{EXT}}^2)_g = (v_{\text{EXT}}^2)_g = 0$. Thus, the A contribution to $\ln(f_c/f_g)^*$ or $\ln(f_p/f_g^2)$ is necessarily positive, i.e., in the direction of a normal isotope effect (light > heavy). The B terms, on the other hand, involve the sum of dimer–monomer or condensed-vapor isotopic frequency differences and can be either positive or negative depending on the sign of the net frequency shift on the phase transfer [i.e., whether it is to the red (negative) or to the blue (positive)]. For monatomic species $B_c = B_p = 0$ (there are no internal modes), and the isotope effects are necessarily positive (normal) since $A_c > 0$ and $A_p > 0$. Alternatively, for molecules with structure the situation is more complicated. If the net shift in internal modes on condensation/dimerization is to the blue, the A and B terms are both positive and reinforce one another. The IE will be positive and large. More often, however, the net shift in isotope sensitive internal frequencies is to the red (the ordinary case for noncomplexed H/D substitution in, for instance, hydrocarbons) and B is of opposite sign to A . Over some range of temperature, B/T may be, and often is, larger in magnitude than A/T^2 . In such cases, the net isotope effect will be negative (inverse), it is a small difference between competing positive and negative terms with distinctly different temperature dependences. These matters have been thoroughly discussed so far as application to VPIE is concerned.^{12,14,17} It is our anticipation that similar considerations will carry over in the interpretation of $(-\text{VCIE})$. This is the principal point of concern for the present paper.

Comparisons of $\ln(f_c/f_g)^$ and $\ln(f_p/f_g^2) = (-\text{VCIE})$.* The important qualitative features of the model introduced above^{14,25} are summarized in Figure 1 and then illustrated for specific examples (methane, water) in Table 1. When a molecule is transferred from its ideal gas reference state to the dimer, or to the condensed phase, significant changes occur in both its internal and external degrees of freedom. In the description of this process (implied in eqs 4 through 12), one refers to a $3n$ dimensional potential energy surface, PES, which describes how

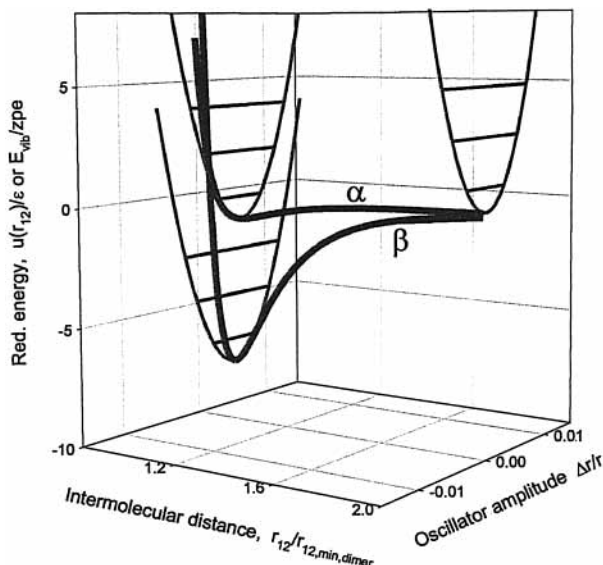


Figure 1. Schematic projection of the $3n$ dimensional (per molecule) potential energy surface describing the effect of intermolecular interaction. The diagram is scaled to approximately represent methane–methane interaction (Table 1). The LJ potential energy of interaction is plotted against intermolecular separation in one plane, the shifts in the position of the minimum, and the curvature of the symmetric CH stretching mode is plotted in another. The heavy upper curve marked α represents the gas–gas “pair” interaction, the lower heavy curve marked β represents condensation. The lighter parabolic curves show the CH stretch internal vibration in the dilute gas, the dimer, and the condensed phase. In each case, the first few vibrational levels, $n_{01} = 3143.7 \text{ cm}^{-1}$ (dilute gas) are shown. At 300 K, RT corresponds to $\sim 8\%$ of the oscillator zpe and $\sim 210\%$ of the LJ well depth (gas phase).

the molecular potential energy depends on the distortion of various atoms or groups of atoms from their respective equilibrium configurations (internal degrees of freedom), and on the position or orientation of the molecule itself (external degrees of freedom). Figure 1 is a representation that shows the shifts in intermolecular potential energy (less vibrational contribution)

and in the internal vibrational potential energy for a single normal mode (specified in terms of bond length, r , or combination of bond lengths and angles as appropriate), as two or more molecules vary their distance of intermolecular separation $R_{\text{INTERMOL}} = R_{12}$. A similar diagram can be constructed for each of the $3n - 6$ internal degrees of vibrational freedom of the molecule of interest. In Figure 1, the upper curve labeled “ α ” sketches the transfer between the dilute gas reference state (on the right at large R_{12}) and the complexed (dimerized) vapor molecule at the bottom of the upper well to the left. Similarly, the lower curve labeled “ β ” shows the transfer from dilute vapor to condensed phase. Thus, while in the first case, $u(R_{12})$ represents the pair intermolecular potential energy, in the second, it represents the projection on the r axis of the average intermolecular potential energy that a single molecule feels when embedded in the field of $(N - 1)$ molecules. The interaction in the condensed phase is with c nearest neighbors (and $(N - c - 1)$ more distant neighbors), and that accounts for the significantly deeper and sharper well which describes condensation. During the change from dilute gas to condensed phase, $\text{PES}_{\text{INTERMOL}}$ shifts to lower energy, and, of at least equal importance, the curvature in the intramolecular dimension is perturbed by virtue of the coupling between internal and external degrees of freedom induced by intermolecular interaction. On condensation, one thus expects, and observes, small changes in the vibrational frequencies of the internal degrees of freedom. Many examples of such frequency shifts, albeit small, have been studied spectroscopically. Increased curvature on condensation corresponds to a blue shift, decreased curvature corresponds to a red shift. Motions along the external degrees of freedom are also quantized but these necessarily correspond to blue shifts, because for these modes in the ideal gas reference state ($\partial^n E_{\text{POT}} / \partial R_{12}^n = 0$ for derivatives of all order).

To recapitulate, within the precision of the Born–Oppenheimer approximation, properly calculated PESs are isotope independent, but the quantized energy states of the motions on the surface are isotope dependent because of isotopic mass differences. Figure 1 illustrates the truism that the intermolecular

TABLE 1: Thermodynamic Properties, Oscillator Energies, and Shifts on Condensation for CH_4 , and CD_4 , and H_2O , and D_2O , Harmonic Oscillator Approximation^a

	CH_4	CD_4	ref or note	H_2O	D_2O	ref
$E_{\text{int(gas)}} = \sum N h c \nu_{\text{int}} [1/2 + 1/(e^{hc\nu/kT} - 1)]$	118 592	87 529	32	53 889	39 768	34
$E_{\text{int(liq)}} = \sum N h c \nu_{\text{int}} [1/2 + 1/(e^{hc\nu/kT} - 1)]$	118 141	87 168	32	52 199	38 297	34
$\delta E_{\text{int}} = (E_{\text{int(gas)}} - E_{\text{int(liq)}})$	451	361	<i>b</i>	1690	1471	
$\Delta \delta E_{\text{int}}$		90	<i>b</i>		219	
$E_{\text{ext(gas)}} = \sum N h c \nu_{\text{ext}} [1/2 + 1/(e^{hc\nu/kT} - 1)]$	0	0	32	0	0	34
$E_{\text{ext(liq)}} = \sum N h c \nu_{\text{ext}} [1/2 + 1/(e^{hc\nu/kT} - 1)]$	5991	5854	32	19 116	17 658	34
$\delta E_{\text{ext}} = (E_{\text{ext(gas)}} - E_{\text{ext(liq)}})$	-5991	-5854		-19 116	-17 658	
$\Delta \delta E_{\text{ext}}$		-137			-1458	
$\delta E_{\text{VAP}} = \delta H_{\text{VAP}} - RT$	7230	(7277)	33, <i>c</i>			
$T = 111.7 \text{ K}$						
$T = 313.15 \text{ K}$				40 745	(41 984)	35, <i>c</i>
$\Delta \delta E_{\text{VAP}}$						
$T = 111.7 \text{ K}$		-47	<i>d</i>			
$T = 313.15 \text{ K}$						
$\delta \epsilon_{\text{liq}} = (\epsilon_{\text{gas}}^{\circ} - \epsilon_{\text{liq}}) = -\delta E_{\text{int}} - \delta E_{\text{ext}} + \delta E_{\text{VAP}}$	12 770	(12 770)	<i>c, f</i>	58 171	(58 171)	<i>c, f</i>
$\delta \epsilon_{6,12,\text{gas}} = (\epsilon_{\text{gas}}^{\circ} - \epsilon_{\text{gas,dimer}}) = Nk(\epsilon/k)_{\text{LJ},6-12}$	1197	(1197)	11, <i>c</i>	3160	(3160)	11, <i>c, g</i>
$\delta \epsilon_{6,12,\text{gas}} / \delta \epsilon_{\text{liq}}$	0.09	(0.09)	<i>f</i>	0.05	(0.05)	<i>f</i>
$(\kappa_d / \kappa_c)_{\text{INTERMOL}}$	0.2	(0.2)				
$\nu_{\text{d,LJ}} / \text{cm}^{-1}$	44			96		<i>g</i>

^a All values in (J mol^{-1}), except for entries otherwise specified. ^b $\delta = (\text{gas} - \text{liquid})$, $\Delta = (\text{light isotope} - \text{heavy isotope}) = (\text{H} - \text{D})$. ^c Parenthesized values are not independent. ^d This is within 7% of the value obtained in ref 19 from the temperature coefficient of the VPIE, -44 J/mol . ^e Within 6% of the value obtained from the temperature coefficient of the VPIE (Table 25, ref 14), -1310 J/mol . ^f This work. ^g The value is that quoted in ref 11 for the Stockmayer potential and does not include any contribution from H-bonding. It is therefore quite unrealistic. ^h Using eq 53 of ref 28 with $c = 10$, $m = 6$, $n = 12$, $s_m = 1.2198$ and $s_n = 1.0092$.

interactions accounting for $\ln(f_p/f_g^2)$ (upper curve) and $\ln(f_c/f_g)^*$ (lower curve) differ not in kind, but in degree. One concludes that $[\ln(f_p/f_g^2)] = (-\text{VCIE})$ should be roughly proportional to $\ln(f_c/f_g)^*$, and the constant of proportionality should be less than unity (because of differences in the well depths and curvatures of the effective intermolecular potentials). The well depth which describes the gas–gas (dimer) interaction is “available” from fits of the second virial coefficient of the parent molecule, and that for the condensed (liquid) phase can be obtained by combining measured energies of vaporization with the zero point energies of the condensed and ideal vapor phases. Typically, for substances with attractive forces limited to the vdW dispersion interaction, $\epsilon_{\text{DIMER}}/\epsilon_{\text{CONDENSED}} \sim 0.1$,²⁸ ϵ_{DIMER} is the well depth of the potential describing the monomer–monomer interaction in the gas, and $\epsilon_{\text{CONDENSED}}$ is the well depth describing the net (sum) of monomer–monomer interactions in the condensed phase (see Figure 1).

Moelwyn-Hughes,²⁸ following Lennard-Jones and Ingham,²⁹ compares the effective intermolecular potential energy in gas and liquid using the general form $u(R_{12}) = C_{12}/R_{12}^n - C_6/R_{12}^m$ (for the Lennard-Jones potential $n = 12$ and $m = 6$). In the condensed phase the interaction is with a set of c nearest neighbors, c' = next-nearest neighbors, etc., and the average potential energy per molecule in a condensed system of N molecules becomes $u(R_{12}) = (s_n C_{12}/R_{12}^n - s_m C_6/R_{12}^m)c/2$ where s_m and s_n are tabulated constants obtained from lattice or smeared lattice sums. Using the (gas + gas = dimer) interaction as reference, he finds the effect of condensation is to bring the molecules some 3 to 5% closer and to increase the well depth by nearly an order of magnitude, at the same time increasing the curvature at the bottom of the intermolecular well (i.e., increasing force constants of the equivalent harmonic oscillators, $k_c > k_d$) and shifting the associated external frequencies commensurately ($\nu_d/\nu_c \sim (1/2.7)^{1/2} \sim 0.6$, and $\nu_d^2/\nu_c^2 = (k_d/k_c)(\mu_c/\mu_d) \sim 0.4$). In the condensed state, the average potential energy is greater than the near pairs value, $(c/2)\epsilon_{\text{DIMER}}$ by 40 to 60% or more.^{28,30,31} These estimates are not claimed to be precise, but they do serve to establish the general features of the effect. In addition, *and importantly for present purposes*, one expects the net internal/external interaction that results in the ZPE shift of internal frequencies and that makes an important contribution to the isotope effects to scale similarly. Two examples (methane^{32,33} and water^{34,35}) are given in Table 1. Summing up, the arguments reviewed above lead us to expect $\ln(f_p/f_g^2)$ to be roughly proportional to $\ln(f_c/f_g)^*$; $\ln(f_p/f_g^2) \sim \chi \ln(f_c/f_g)^*$, with the proportionality constant $\chi \sim 0.2 \pm 0.1$.³⁶ A more detailed description of the application of the Lennard-Jones Ingham model to molecules discussed in this paper is outlined in a later section.

The discussion based on the Lennard-Jones Ingham model, strictly interpreted, refers to intermolecular modes only. With modest generalization, we expect similar arguments to apply to intramolecular modes as well. In that case, the intermolecular and intramolecular (external and internal) contributions to $\ln(f_p/f_g^2)$ and $\ln(f_c/f_g)^*$ should separately correlate with proportionality constants $\chi(\text{internal}) \sim \chi(\text{external}) \sim 0.2 \pm 0.1$. Most commonly, however, internal and external contributions to $\ln(f_p/f_g^2)$ and $\ln(f_c/f_g)^*$ are of opposite sign and are usefully described using the A,B formalism, eqs 12a and 12b discussed above. The ratio $[\ln(f_p/f_g^2)/\ln(f_c/f_g)^*] = [A_p/T^2 + B_p/T]/[A_c/T^2 + B_c/T]$, is zero at the crossover temperature for $(-\text{VCIE})$, $T_{\text{CROSS,p}} = -A_p/B_p$, and is unbounded at the crossover temperature for $\ln(f_c/f_g)^*$, $T_{\text{CROSS,c}} = -A_c/B_c$. By crossover is meant that temperature at which one or the other isotope effect, \ln

(f_p/f_g^2) or $\ln(f_c/f_g)^*$, goes through zero and changes sign. Thus, at temperatures near either crossover we conclude it is rather more useful to report ratios of each of the A and B parameters and not ratios of the overall effects.

Comparisons of Experimental VCIE and VPIE Data.

Tables 2 and 3 review data for most of the 14 compounds (24 sets of isotopomer pairs) for which experimental data on both VCIE and VPIE are available.^{5–8,27,32,34,37–50} Virial coefficients have been tabulated by Dymond and Smith.³⁷ Jancso and Van Hook¹⁴ reviewed VPIE data in 1974. The VCIEs of two isotopomer pairs, $\text{C}_6\text{H}_6/\text{C}_6\text{D}_6$ ⁵⁰ and $\text{CH}_3\text{OH}/\text{CH}_3\text{OD}$,⁵⁰ are reported at a precision too low to permit the data to be usefully included in the correlations. Another two pairs, H_2/D_2 and He^3/He ,⁴ are very light; quantum corrections are large and the thermodynamics are complicated by nuclear spin effects. These systems will not be considered in this paper.

Figures 2 and 3 contain plots that compare low-temperature $\ln(f_c/f_g)^*/\Delta M$ with $[\ln(f_p/f_g^2)/\Delta M = (-\text{VCIE})/\Delta M]$ for 19 of the remaining 20 pairs (nine different compounds). For the remaining pair, HCl/DCl , $\text{VCIE} = 0$ and a plot is uninformative.^{51–53} In every case, $\ln(f_p/f_g^2)$ has been measured at appreciably higher temperatures (sometimes well above T_c) than has $\ln(f_c/f_g)^*$, and the comparison is effectively one between the least-squares parameters A_c and B_c deduced from least-squares fits of $\ln(f_c/f_g)^*$ vs T , for $T_r < \sim 0.7$ (eq 12b) and A_p and B_p from fits of $\ln(f_p/f_g^2)$ at higher temperature, sometimes for $T_r > 1$. We have chosen to express the IEs in terms of $[\ln(f_c/f_g)^*/\Delta M]$ and $[\ln(f_p/f_g^2)/\Delta M]$ for economy of presentation. We are aware that deviations from the rule of the geometric mean, well understood in the case of the $\ln(f_c/f_g)^*$,^{12–14} and certainly expected for $\ln(f_p/f_g^2)$, imply this representation to be approximate. However, the rather large imprecision of VCIE measurements (as compared to $\ln(f_c/f_g)^*$) introduces an uncertainty larger than that involved in deviations from the rule of the mean. In fact, on the scale of the figures, only for the very light series $[\text{CH}_4\dots\text{CD}_4]$ are deviations of VPIE from the geometric mean apparent (Figure 3a).

In Figures 2 and 3, one notes that in almost every case $\ln(f_p/f_g^2)$ is of the same sign and smaller in magnitude, yet commensurate, with $\ln(f_c/f_g)^*$. The virial coefficient data are consistent with the VPIE correlation expected from the discussion above. Both effects, VPIE and $(-\text{VCIE})$, $\ln(f_c/f_g)^*$ and $\ln(f_p/f_g^2)$, are subject to the same underlying theoretical principles, and that is the most important point of concern in the present paper. (That in mind, we remark that it is unfortunate that almost all VCIE data lie at much higher temperature than do the experimental VPIE data used to define $\ln(f_c/f_g)^*$. We recommend future VCIE measurements at lower T where direct comparison with measured values of $\ln(f_c/f_g)^*$ obtained from VPIE becomes possible. Low-pressure/low-temperature VCIE measurements will be difficult, but experiments in this regime should permit a more specific and detailed theoretical description of $\ln(f_p/f_g^2)$. In Table 2, we report (A,B) parameters of fit to eq 6 for averaged $\ln(f_c/f_g)^*/\Delta M$ and $\ln(f_p/f_g^2)/\Delta M$ data. In some cases, VCIE scatters badly, and it is impossible to define two parameters with meaningful statistical precision. For H-bonded systems, the statistical quality of the two parameter fits is in excess of $r^2 = 0.9$ (r^2 is the coefficient of determination, r is the correlation coefficient⁵⁴), but the statistical quality of the hydrocarbon measurements is not as good. These caveats in mind, we calculated $[\ln(f_p/f_g^2)/\ln(f_c/f_g)^*]$ ratios for A and B parameters. Despite large uncertainties, the averaged ratios, $\langle(A_p/A_c = A_{\text{VCIE}}/A_{\text{VPIE}})\rangle = 0.4 \pm 0.2$ and $\langle(B_p/B_c = B_{\text{VCIE}}/B_{\text{VPIE}})\rangle = 0.3 \pm 0.2$,

TABLE 2: Review of Isotope Effect Data and Correlating Equations Used in This Paper^a

isotopic pair	$(-VCIE) = \ln(f_p/f_g^2)$					$(VPIE) = \ln(f_c/f_g)^*$					
	ndp ²	$A_p/\Delta M$	$B_p/\Delta M$	\sim range K	b_o cm ³	ref	$A_c/\Delta M$	$B_c/\Delta M$	range K	$T_{CRITICAL}^c$	ref
Ar ³⁶ /Ar ⁴⁰	3	10.4		120/273	50	38	10.4		84/150	151	14, 22, 56
CH ₃ F/CD ₃ F	3	184		218/273	80	37	512		130/210	318	39
CH ₄ /CH ₃ D	4	<i>c</i>		110/300		5, 37	<i>d</i>				
CH ₄ /CH ₂ D ₂	4	<i>c</i>		110/300		5, 37	<i>d</i>				
CH ₄ /CHD ₃	4	<i>c</i>		110/300		5, 37	<i>d</i>				
CH ₄ /CD ₄	21	<i>c</i>		110/500		5, 6, 37	<i>d</i>				
CH ₄ / all D isomers	33	233 ± 40	-2.34 ± 0.21		70.2	5, 6, 37	258	-2.89	90/120	191	14, 32
C ₂ H ₄ /C ₂ H ₂ D ₂ -tr	6	<i>c</i>		200/273		8, 37	<i>d</i>				
C ₂ H ₄ /C ₂ H ₂ D ₂ gem	2	<i>c</i>		200/210	8, 37	<i>d</i>					
C ₂ H ₄ /C ₂ D ₄	13	<i>c</i>		210/300	7, 8, 37	<i>d</i>					
C ₂ H ₄ /all D isomers	21	97 ± 60	-0.91 ± 0.26		117		327	-3.28	115/180	283	14
C ₂ H ₆ /C ₂ D ₆	8	53 ± 23	-0.74 ± 0.08	210/520	78	7, 37	140	-2.86	115/200	305	14
C(CH ₃) ₄											
/C(CH ₃) ₃ (CD ₃)	5	<i>c</i>		345/510		7, 37					
/C(CH ₃) ₂ (CD ₃) ₂	6	<i>c</i>		345/510		7, 37					
/C(CH ₃) ₃ (CD ₃)	6	<i>c</i>		345/510		7, 37					
/C(CH ₃) ₂ (CD ₃) ₂	5	<i>c</i>		315/510		7, 37					
C(CH ₃) ₄ /all D isomers	22	10.2 ± 5.1	-0.51 ± 0.13		300		-117	-1.42	257/293	434	14
NH ₃ /ND ₃	7	2630 ± 124	-5.43 ± 0.34	298/473	22.1	37	5320	-12.2	218/273	406	14
CH ₃ NH ₂ /CH ₃ ND ₂	9	1960 ± 382	-2.70 ± 1.00	298/540	80	37	5120	-11.8	218/298	430	14
CH ₃ NH ₂ /CD ₃ NH ₂	10	-642 ± 150	0.31 ± 0.30	298/515	80	37	-164	-2.38	218/293		14
CH ₃ NH ₂ /CD ₃ ND ₂	8	340 ± 44	-0.83 ± 0.12	298/515	80	37	2100	-6.64	218/293		14
HCl/DCI	3	(-VCIE = 0)		190/290		37, 47	3910	-17.6	160/225	325	46
H ₂ O/D ₂ O	11	4277	-6.14	473/723	24.6	49	16900	-35.2	273/423	647	14

^a The correlating equations in this table report smoothing equations drawn through the plots of VPIE or -VCIE data (see Figures 2 and 3) according to eq 6. For VPIE, high experimental precision often requires a more elaborate form (refer to original literature) if fitting within the experimental precision is desired. In some cases, poor precision of (-VCIE) results in large uncertainties in A and B parameters. ^b ndp = no. of data points. ^c Fits to individual isotopomer pairs not available for (-VCIE). An estimate of the reliability of fit can be made by examining Figures 2 and 3. ^d Fits to individual isotopomer pairs are available in the references. The precision of these VPIE data is \sim 100 times that for (-VCIE) and in some cases require fitting equations that are more elaborate than eq 6. Large deviations from the rule of the geometric mean for the VPIE are observed for the deuteromethanes, ethanes, and ethylenes. Detailed consideration of such higher order effects is not appropriate in comparisons with (-VCIE) data which are of much lower precision. ^e $T_{CRITICAL}$ refers to the common isotope.

TABLE 3: Review of Correlating Equations Used in This Paper to Describe $\mathcal{B}(T)^a$

gas	A	B	C	b_o
Ar ⁴⁰	1.37	142	-4020	50
CH ₃ F ^b	-794	4.36 × 10 ⁵	8.27 × 10 ⁷	80
CH ₄	1.53	175	-6460	70.2
C ₂ H ₄	1.79	221	-10 700	117
C ₂ H ₆	1.49	363	-25 700	78
C(CH ₃) ₄	2.28	242		300
NH ₃	1.17	384		22.1
CH ₃ NH ₂	1.91	174	21 200	80
H ₂ O	0.950	717	-15 900	24.6

^a Correlating parameters for $\log[-(\mathcal{B}(T) - b_o)] = A + B/T + C/T^2$. $\mathcal{B}(T)$ data from ref 37 for temperature range given in Table 2. The units of $\mathcal{B}(T)$ and b_o are cm³/mol; b_o from standard compilations.¹¹

^b These parameters for fit to $[-(\mathcal{B}(T) - b_o)] = A + B/T + C/T^2$ (rather than to $\log[-(\mathcal{B}(T) - b_o)]$).

are consistent with the expectations of the model. We believe that the large uncertainties observed for these ratios are a consequence primarily of experimental uncertainty in the VCIE data. This matter is more thoroughly discussed below in the section Discussion: General Remarks.

Figure 4 shows another test of the correlation between $\ln(f_c/f_g)^*$ and $[-VCIE]$. Here we compare $\ln(f_p/f_g^2)$ near the midrange of measurement, $1.5T_b$, with $\ln(f_c/f_g)^*$ at the boiling temperature, T_b . The correlation line is $[\ln(f_p/f_g^2)]_{1.5T_b} = 0.165[\ln(f_c/f_g)^*]_{T_b} - 0.00103$, $r^2 = 0.77$. The point with the largest deviation from the line refers to the methane/deuteromethane system, which includes the molecules most sensitive to rotational contributions (A term). A more direct comparison (since it refers to identical

temperatures) is given in Figure 5. The figure plots experimental values of $[\ln(f_p/f_g^2)/\Delta M]$ vs $[\ln(f_c/f_g)^*/\Delta M]$. An equation for the reasonably good linear correlation is reported in the caption. The correlations in Figures 4 and 5 are consistent with the general features of the Lennard-Jones Ingham model.²⁸⁻³¹ Within the statistical error, which is large, the parameters lie within the expected range.

In the $\ln(f_c/f_g)^*/\ln(f_p/f_g^2)$ comparisons made in this section and throughout the paper, it is important to keep several caveats in mind. To begin, eq 5, widely used for interpretation of VPIE data when approximated with the A/B formalism eq 12b, is only valid at pressures low enough to ignore PV correction terms (see eqs 4 and 5). Similarly eqs 10, 11, and 12b which refer to (-VCIE) are limited to pressures where contributions from third and higher virial coefficients are negligible. In the present context, however, we are comparing $\ln(f_p/f_g^2)$ and $\ln(f_c/f_g)^*$ at pressures and temperatures low enough to avoid such complication. This we have accomplished by restricting the VPIE data used to define $\ln(f_c/f_g)^*$ to low temperature and low to modest pressure, $\ln(f_c/f_g)^* = A_c/T^2 + B_c/T \sim$ VPIE, comparing with (-VCIE) at higher temperature, but still low to modest pressure, $\ln(f_p/f_g^2) = A_p/T^2 + B_p/T$. In this fashion, we avoid all regions of the phase diagram with large PV corrections for either phase. The comparison that interests us is that between the linear combination of temperature scaled fitting parameters, $[A_c/T^2 + B_c/T]/[A_p/T^2 + B_p/T]$, always at low or modest pressure. In no sense can or do we claim to directly compare vapor pressures and VPIEs, with virial coefficients and VCIEs, at temperatures near or above the critical temperature, or at high pressure.

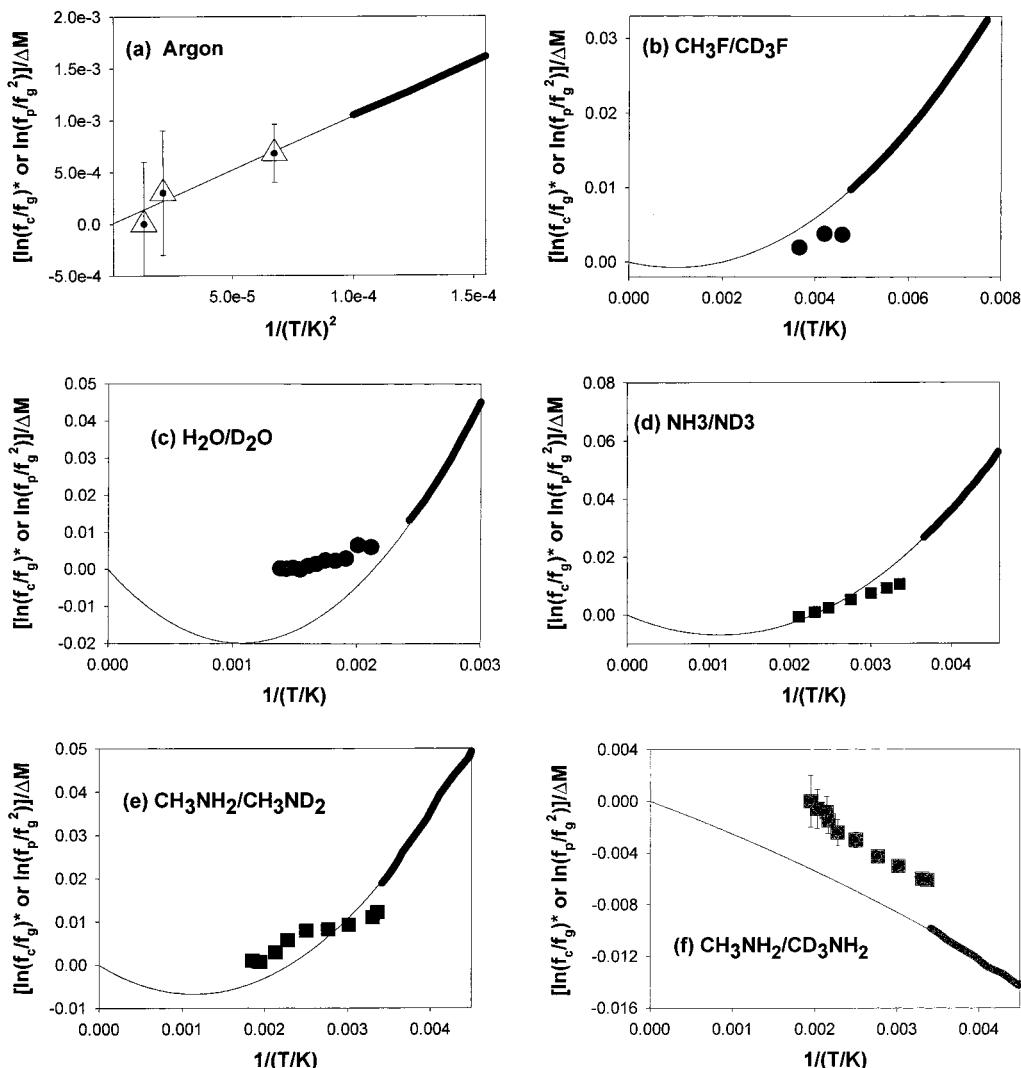
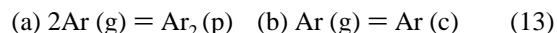


Figure 2. Comparisons of $\ln(f_p/f_g^2) = (-\text{VCIE})$ and low-temperature VPIE data, $\ln(f_c/f_g)^*$, $T/T_{\text{CRITICAL}} < \sim 0.7$, for some non-hydrocarbons. $\ln(f_p/f_g^2)$ data points are shown as the large symbols. Smoothed values for $\ln(f_c/f_g)^*$ are plotted as solid lines, the heavy portion of which shows the range of the original data selected to define $\ln(f_c/f_g)^*$; the lighter portion, a guide to the eye only, is obtained from eq 6. In every case, $\ln(f_c/f_g)^*$ experimental data are far more precise than $\ln(f_p/f_g^2)$, see Table 2. Parameters of fit to $\ln(f_c/f_g)^*$, $\ln(f_p/f_g^2)$, and literature citations are reported in Table 2. (a) $^{36}\text{Ar}/^{40}\text{Ar}$, (b) $\text{CH}_3\text{F}/\text{CD}_3\text{F}$, (c) $\text{H}_2\text{O}/\text{D}_2\text{O}$, (d) NH_3/ND_3 , (e) $\text{CH}_3\text{NH}_2/\text{CH}_3\text{ND}_2$, (f) $\text{CH}_3\text{NH}_2/\text{CD}_3\text{NH}_2$. Not included is a diagram for $\text{CH}_3\text{NH}_2/\text{CD}_3\text{ND}_2$ because within experimental precision both $(-\text{VCIE})$ and VPIE for this pair are given by $\{[\text{CH}_3\text{NH}_2/\text{CD}_3\text{NH}_2] + [\text{CH}_3\text{NH}_2/\text{CH}_3\text{ND}_2]\}$.

Discussion

General Remarks. The ratio, $[(\ln(f_p/f_g^2)/\ln(f_c/f_g)^*)] \sim 0.4 \pm 0.2$, observed for a wide series of compounds (at temperatures well removed from either crossover) is consistent with that expected from the Lennard-Jones and Ingham model, $\sim 0.2 \pm 0.1$.^{30,36} Both $\ln(f_c/f_g)^*$ and $\ln(f_p/f_g^2)$ depend on temperature in a complicated fashion, $\ln(R_{\text{VPIE or VCIE}}) = A/T^2 + B/T$. For many compounds, the A and B terms are of opposite sign but of commensurate magnitude; in these cases, $\ln R$ amounts to a small difference between much larger terms. It is this difficulty, compounded by experimental uncertainty in the VCIE data, which probably accounts for the major part of the error in the correlations reported above. Further progress in refining ideas concerning the comparison between $\ln(f_c/f_g)^*$ and $\ln(f_p/f_g^2)$ awaits (1) improved VCIE data of high precision, extending when possible to temperatures which overlap $\ln(f_c/f_g)^*$ and/or (2) detailed spectroscopic information on pressure broadening and pressure shifts of isotope sensitive vibrational frequencies. The spectroscopic data should permit detailed calculation of $B_p = B_{\text{VCIE}}$ using well established methods successfully developed for the interpretation of VPIEs.^{13–14,16–18}

Approximate Model Comparisons of $\ln(f_p/f_g^2)$ and $\ln(f_c/f_g)^*$. *Argon.* Consider the interaction of two monatomic (argon) atoms in the gas (eq 13a) or the condensation of one atom (or mole) of argon (eq 13b),



For monatomic argon, there are no internal frequencies, so eq 12a for $\ln(f_p/f_g^2)$ and its analogue eq 12b for $\ln(f_c/f_g)^*$ reduce to one-term expressions

$$(a) \ln(f_p/f_g^2) = A_p/T^2 \quad \text{and} \quad (b) \ln(f_c/f_g)^* = A_c/T^2 \quad (14)$$

In each case, the B parameter is zero.

Now compare gas–gas dimerization (eqs 13a and 14a) with condensation into the liquid “lattice” (eqs 13b and 14b). On the left of eq 13a, 6 translational degrees of freedom (unhindered and thus corresponding to null frequencies) yield, on the right, 3 gas-phase dimer translations and 2 dimer rotations (null frequencies), plus 1 internal dimer vibration. We follow Moelwyn-Hughes²⁸ in using the harmonic approximation, ν_d

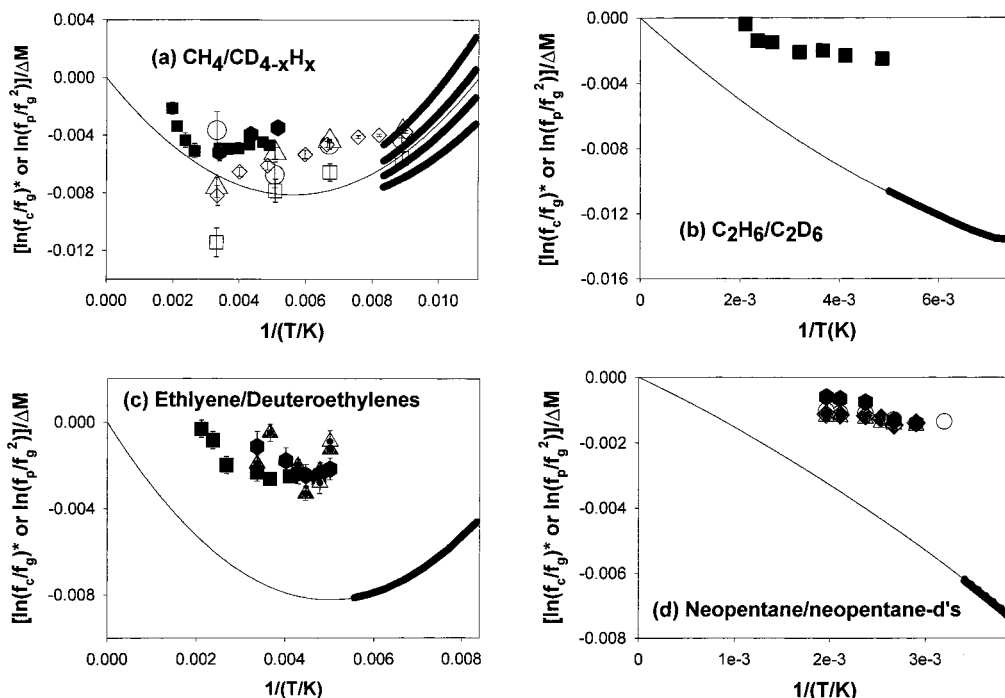


Figure 3. Comparisons of $\ln(f_p/f_g^2) = (-\text{VCIE})$ and low-temperature VPIE data, $\ln(f_c/f_g)^*$, $T/T_{\text{CRITICAL}} < \sim 0.7$, for some hydrocarbons. $\ln(f_p/f_g^2)$ data points are shown as the large symbols. Smoothed values for $\ln(f_c/f_g)^*$ are plotted as solid lines, the heavy portion of which shows the range of the original data selected to define $\ln(f_c/f_g)^*$; the lighter portion, a guide to the eye only, is obtained from eq 6. In every case, $\ln(f_c/f_g)^*$ experimental data are far more precise than $\ln(f_p/f_g^2)$, see Table 2. Parameters of fit to $\ln(f_c/f_g)^*$, $\ln(f_p/f_g^2)$, and literature citations (when not specified below) are reported in Table 2. (a) Methane/deuteromethanes: $\text{CH}_4/\text{CH}_3\text{D}$ (circles⁵), $\text{CH}_4/\text{CH}_2\text{D}_2$ (squares⁵), CH_4/CHD_3 (triangles⁵), and CH_4/CD_4 (diamonds,⁵ hexagons,⁶⁴ and squares⁶). The four separate curves for $\ln(f_c/f_g)^*$, (reading down, in order) $\text{CH}_4/\text{CH}_3\text{D}$, $\text{CH}_4/\text{CH}_2\text{D}_2$, CH_4/CHD_3 , and CH_4/CD_4 , demonstrate well understood large deviations from the rule of the geometric mean.³² (b) $\text{C}_2\text{H}_6/\text{C}_2\text{D}_6$. (c) $\text{C}_2\text{H}_4/\text{C}_2\text{D}_4$ (squares⁵ and triangles⁵), $\text{C}_2\text{H}_4/\text{trans-C}_2\text{H}_2\text{D}_2$ (hexagons⁸) and $\text{C}_2\text{H}_4/\text{gem-C}_2\text{H}_2\text{D}_2$ (triangles⁸). (d) $\text{C}(\text{CH}_3)_4/\text{C}(\text{CH}_3)_3(\text{CD}_3)$ (hexagons), $\text{C}(\text{CH}_3)_4/\text{C}(\text{CH}_3)_2(\text{CD}_3)_2$ (triangles), $\text{C}(\text{CH}_3)_4/\text{C}(\text{CH}_3)(\text{CD}_3)_3$ (diamonds), and $\text{C}(\text{CH}_3)_4/\text{C}(\text{CD}_3)_4$ (circles).

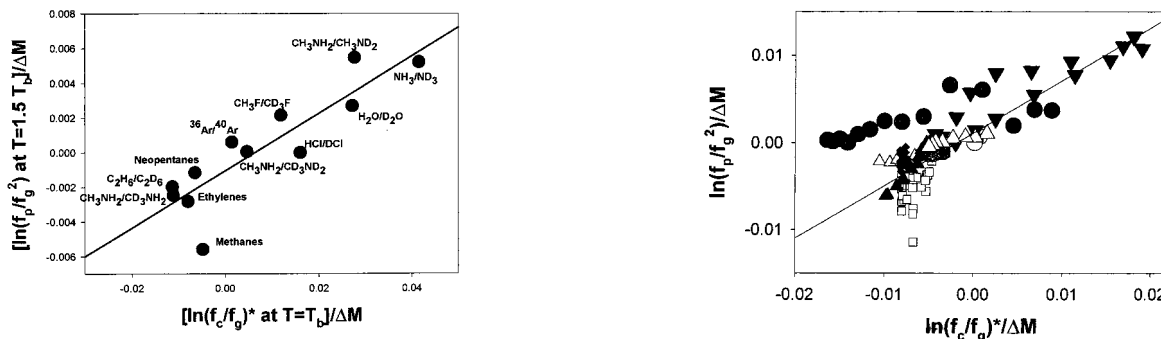


Figure 4. The correlation of $\ln(f_p/f_g^2) = (-\text{VCIE})$ near the midrange of its measurement ($\sim 1.5T_b$) with $\ln(f_c/f_g)^*$ at the boiling point, T_b . The linear correlation line is $\ln(f_p/f_g^2)_{1.5T_b} = 0.165 \ln(f_c/f_g)^*_{T_b} - 0.00103$, $r^2 = 0.77$.

$= 1/(2\pi)(\kappa_p/\mu_p)^{1/2}$ with $1/\mu_d = 1/m_1 + 1/m_2 = 2/m$, where m refers to the masses of the two interacting atoms (both the same), and κ_p is the force constant taken from the curvature at the bottom of the well. For condensation, 3 degrees of gas-phase translational freedom on the left go over to 3 hindered lattice vibrations. The vibration is now against the lattice and $1/\mu_c = 1/m_1 + 1/m_{\text{lattice}} = 1/m$. In either case, κ is the force constant describing the curvature at the bottom of the well and $m_1 = m_2 = m$ are the masses of the interacting particles. Again, following Moelwyn-Hughes,²⁸ as outlined in refs 30 and 31, we obtain ratios of force constants and squared frequencies, $\kappa_c/\kappa_p = 5.3 \pm 0.6$ and $[\nu_c/\nu_p]^2 \sim 2.7 \pm 0.3$, to sufficient precision. In the dimer, there is one frequency per pair of atoms. It is small (vide supra), and the high-temperature approximation is appropriate. $\ln(f_p/f_g^2)$ is proportional to ν_p^2 . In the condensed phase, there is a band of hindered translational frequencies (3 from each

Figure 5. The correlation of $\ln(f_p/f_g^2) = (-\text{VCIE})$ across the range of its measurement with $\ln(f_c/f_g)^*/\Delta M$ at the temperatures of the experimental VCIE measurements. The correlation line is $\ln(f_p/f_g^2) = 0.49 \ln(f_c/f_g)^* + 1.2 \times 10^{-3}$, $r^2 = 0.6$. Open circles = argon; darkly shaded circles = $\text{CH}_3\text{F}/\text{CD}_3\text{F}$; small squares = methanes; lightly shaded triangles = ethanes; small diamonds = ethylenes; shaded hexagons = neopentanes; large inverted triangles = ammonia; large inverted crossed triangles = methylamines (CD_3); upright dotted triangles = methylamines (ND_2); upright open triangles = methylamines (CD_3ND_2); crossed shaded circles = $\text{H}_2\text{O}/\text{D}_2\text{O}$.

condensed phase atom, which, we assume, suitably average to ν_c), so the contribution to $\ln(f_c/f_g)^*$ is proportional to $3\nu_c^2 = 3(2.7 \pm 0.3)\nu_p^2$. With the use of an experimentally available frequency⁵⁵ for Ar_2 (Table 3 of ref 53) and the equations above and in refs 28, 30, and 31, one obtains $\ln(f_p/f_g^2) = [-\text{VCIE}] = (1/24)(hc/k)^2(\nu_p'/T)^2(1-36/40) = 6.3/T^2$ per pair so $\ln(f_p/f_g^2)/\Delta M = 1.6/T^2$. Also, from the development above, $\ln(f_c/f_g)^* = 3(2.7 \pm 0.3) \ln(f_p/f_g^2) = (46 \pm 5)/T^2$, $(\ln(f_c/f_g)^*/\Delta M) = (12 \pm 1)/T^2$. The value extracted from the Lee-Bigeleisen experimental data⁵⁶ is $A_c/\Delta M = 10.4 \text{ K}^2$, and is in reasonable agreement with

TABLE 4: Parameters Employed for LJ Estimates of $A_p/\Delta M = A_{(-VCIE)}/\Delta M$ and $A_c/\Delta M = A_{VPiE}/\Delta M$ for Four Systems

system	(ϵ/k) K	σ/A	ν_p cm^{-1}	ν_c cm^{-1}	$A_{(-VCIE)}$ K^2	A_{VPiE} K^2	remarks
Ar ³⁶ /Ar ⁴⁰	118 ⁵⁷	3.4 ⁵⁷	26		1.6		<i>a</i>
expt ⁵⁵⁻⁵⁷			26	47 ± 5 41	10	12 10	
methane/ deutero- methanes							
calc (I)	148 ¹¹	3.82 ¹¹	44	44	113	238	<i>a, b</i>
(II)			44	72	288		
expt				75	233 ± 40	258	
C ₂ H ₆ /C ₂ D ₆							
calc (I)	243 ¹¹	3.95 ¹¹	40	69	42	132	<i>a, c</i>
(II)					90	132	
expt					53 ± 23	140	
C ₂ H ₄ / deutero ethylenes							
calc (I)	199 ¹¹	4.52 ¹¹	33	57	38	94	<i>a, d</i>
(II)					74	206	
expt					97 ± 60	327	

^a See text for a thorough discussion. ^b Calc. I and Calc. II differ in the treatment of the rotational contribution for the gas dimer, see text. ^c Calc(I) $\nu(\text{rot,dimer}) = \nu(\text{tr,dimer})$, $\delta\nu(\text{int rot}) = 0$; Calc(II) as Calc(I) except $\delta\nu(\text{int rot}) = \delta\nu(\text{int rot, liq}) = (290-278)$. In either case, there is rough correspondence between vpie and (-vcie) and the model. ^d Calc(I), $\nu(\text{rot,dimer}) = \nu(\text{tr,dimer})$; Calc(II) as Calc(I) except $\nu(R_c)/\nu(R_e) = 2.1$ which was the value used in VPiE liquid-state calculations.¹⁴

this estimate, 12 K². Presumably, proper consideration of anharmonicity in the LJ calculation would improve the agreement.

It is interesting to compare experimentally available frequencies⁵⁵ for Ar₂. The observed frequency for the lowest transition is $\nu_{1,0} = 25.7 \pm 0.5 \text{ cm}^{-1}$, but the potential is highly anharmonic, (for instance $\nu_{2,1} = 20 \text{ cm}^{-1}$). Using LJ parameters from Hirschfelder, Curtiss and Bird¹¹ (Table 4), we calculate $\nu_{LJ} = 30 \text{ cm}^{-1}$ in good agreement with 25.7 cm^{-1} , but that improves ($\nu_{LJ} = 26$) with use of the more recent values, $\epsilon/k = 117.7 \text{ K}$ and $\sigma = 3.404A$, of Fischer et al.⁵⁷ For the condensed phase, still following Moelwyn-Hughes,²⁸⁻³¹ one obtains ($42 < \nu_c < 52 \text{ cm}^{-1}$); the range is determined by the choice of coordination number and lattice employed in the calculation outlined in footnote 27. An experimental estimate for ν_c is available from $\ln(f_c/f_g)^*$ derived force constants reported by Lee and Bigeleisen.⁵⁶ One obtains temperature-dependent effective harmonic frequencies $\nu_c = 41, 40, 36,$ and 24 cm^{-1} at $T = 85, 95, 120,$ and 150 K (critical point), respectively.^{58,59} Thus, there is reasonable agreement between the LJ estimated and the "experimental" ν_c 's at low temperature ($\sim 47 \pm 5$ vs $41 \pm 2 \text{ cm}^{-1}$) and also at higher temperature (~ 28 vs 24 cm^{-1}). The former comparison is between the LJ estimated condensed phase frequency and the Lee-Bigeleisen low-temperature liquid frequencies, while the latter is between the LJ dimer frequency and the Lee-Bigeleisen value at the critical point. The agreement between the lattice frequencies of the condensed phase calculated using the LJ model, i.e., the ν_c 's, and those obtained from interpretation of the $\ln(f_c/f_g)^*$ data is reassuring. It confirms the validity of the present approach. However, it is puzzling that the value for $\ln(f_p/f_g^2)$ calculated from the LJ dimer frequency in the harmonic approximation (eq 12a and Table 4), crude though it may be, differs appreciably from experimental measurement.³⁸ That difference is worrisome. It has led us to

initiate further studies⁶⁰ that will compare quantum corrections to $[-VCIE]$ for LJ and other potentials using various methods, including those first introduced by deBoer and Michels.²⁶ So far as the harmonic approximation is concerned, however, one expects approximately the same reliability for values calculated from an LJ potential for both $\ln(f_p/f_g^2)$ and $\ln(f_c/f_g)^*$. (VPiE)_{Ex-}perimental is well established by measurements from several laboratories¹⁴ and is in reasonable agreement with calculation. We estimate the precision of the harmonic LJ calculation for $\ln(f_c/f_g)^*$ to be good to within a factor of ~ 2 . $\ln(f_c/f_g)^*$ is reliable to $\sim 5\%$ or better in the temperature range of the experimental VPiE data, ($\sim 85 < T/K < \sim 125$), less reliable at higher temperature ($217 < T/K < 273$) where the comparison with $\ln(f_p/f_g^2)$ is made. Even so, $\ln(f_c/f_g)^*$ is certainly established at high temperature to well within a factor ~ 2 . The error bars in Figure 2a correspond to $\delta\Delta\mathcal{B} = \pm 0.2 \text{ cm}^3/\text{mol}$.

Methane/Deuteromethanes. For molecules with structure, one expects significant contributions to $\ln(f_p/f_g^2)$ from both external (dimer) and internal (vibrational) modes, as was true for $\ln(f_c/f_g)^*$. The (LJ) development outlined above applies only to external modes, and the following discussion is limited to that part of the problem, comparing A/T^2 (eqs 6 and 12) obtained from measurements of VPiE and $(-VCIE)$ with each other and with values obtained from the LJ calculations.^{28,30,31} There is a large isotope effect on the moments of inertia of the deuteromethanes, and rotational effects are expected to be important. In that context, consider dimerization of methane, 2CH_4 (free) = $(\text{CH}_4)_2$ (dimer). As before, 6 translational (null frequencies) and 6 rotational modes (null frequencies) per pair of dilute gas molecules yield 3 dimer translations and 3 dimer rotations (null frequencies), plus 1 methane-methane dimer stretching vibration, 1 methane-methane torsion, and 4 dimer methane-methane bending modes (perhaps better described as hindered internal rotations). The bending modes are presumably characterized by G matrix elements that are more nearly proportional to $1/I$ or $1/I_{\text{RED}}$ than the $1/M$ or $1/\mu$ dependences that describe the methane-methane dimer vibration or condensed phase hindered translations. In summary then, 12 external degrees of freedom per pair of molecules in the dilute gas (null frequencies) yield 6 null frequencies and 6 real frequencies in the dimer. For the dimer vibration, $\nu_d = 1/(2\pi)(\kappa/\mu)^{1/2}$; $1/\mu = 1/m_1 + 1/m_2 = 2/m$ (m is the mass of the methane molecule), while for the internal rotational modes $1/I_{\text{RED}} \sim 1/I_1 + 1/I_2 \sim 2/I$ and $\nu_{\text{ROT}} \sim 1/(2\pi)(2\kappa/I)^{1/2}$. Compare this result with that for condensation where the 6 degrees of translational and rotational freedom per gas-phase molecule go over to 6 hindered lattice vibrations. As for argon, we take $[\nu_c/\nu_p]^2 \sim (2.7 \pm 0.3)$ to sufficient precision. In the gas dimer, there is one vibrational frequency per pair of molecules, and five hindered rotational frequencies (bending modes) per pair. The contribution to $\ln(f_p/f_g^2)$ is proportional to $[\nu^2(\text{vib, dimer}) + 5\nu^2(\text{rot, dimer})]$. In the calculation of $\ln(f_c/f_g)^*$, we consider 6 external frequencies per molecule; the contribution is proportional to $[3\nu^2(\text{vib, lattice}) + 3\nu^2(\text{rot, lattice})]$.

The numerical calculations using LJ parameters from Hirschfelder, Curtiss and Bird¹¹ are summarized in Table 4. Those calculations and the following discussion are limited to consideration of the A/T^2 contributions to $\ln(f_p/f_g^2)$ and $\ln(f_c/f_g)^*$. One obtains $\nu_p(\text{vib,CH}_4) = 44 \text{ cm}^{-1}$, which, assuming $\nu_p(\text{rot}) = \nu_p(\text{vib})$ yields $\ln(f_p/f_g^2)_{\text{CH}_4/\text{CD}_4} = (1/24)(hc/k)^2(\nu_p/T)^2[(1 - 16/20) + 5(1 - 1/2)] = 452/T^2$, or $\ln(f_p/f_g^2)/\Delta M = 113/T^2$. We have followed Bigeleisen Craig and Jeevanandam³² in taking

$\nu^2(\text{vib}) \sim \nu^2(\text{rot})$. Turning attention to $\ln(f_c/f_g)^*$, we obtain, $\ln(f_c/f_g)^* = (2.7)(1/24)(hc/k)^2(\nu_p'/T)^2[3(1 - 16/20) + 3(1 - 1/2)] = 950/T^2$ or $\ln(f_c/f_g)^*/\Delta M = 238/T^2$. The liquid frequency obtained from the LJ calculation is $((2.7 \pm 0.3)44^2)^{1/2} = 72 \pm 4 \text{ cm}^{-1}$, which is in good agreement with the BCJ values, $\nu_c(\text{vib}) = 77 \text{ cm}^{-1}$ and $\nu_c(\text{rot}) = 72 \text{ cm}^{-1}$. Even so, the value obtained for $\ln(f_p/f_g^2)$ from the LJ analysis, $A_p/\Delta M = A_{[-\text{VCIE}]/\Delta M} = 113\text{K}^2$, is not in good agreement with experiment, $233 \pm 40 \text{ K}^2$; it is too small. As in the case of argon, $A_p \sim A_c$, and that observation is difficult to rationalize. In any case, using a somewhat different set of assumptions, taking $\nu_d(\text{vib}) \sim 44 \text{ cm}^{-1}$ as before but assuming $\nu_d(\text{rot}) \sim \nu_c(\text{rot}) = 72 \text{ cm}^{-1}$, one obtains $A_p/\Delta M = 288 \text{ K}^2$, in somewhat better agreement with experiment. The "external" contribution in methane is large. The agreement between the LJ calculation and experiment for $A_c = A_{\text{VPIE}}$ is gratifying, but the use of "liquidlike" rotational frequencies to calculate $A_p = A_{\text{VCIE}}$ is unpalatable even though the result is reasonable.

Brief Comments, Other Species: (a) *Methyl Fluoride* $\text{CH}_3\text{F}/\text{CD}_3\text{F}$. $[-\text{VCIE}]$ is small and positive. The liquid-phase frequency, 55 cm^{-1} , obtained from the LJ parameters, compares with Ishida's³⁹ value $\sim 80 \text{ cm}^{-1}$. The temperature dependence of $\ln(f_c/f_g)^*$ is large, and Ishida and co-workers³⁹ introduced temperature-dependent external frequencies which they attributed to specific directional interactions, dampening as T increases. $(\ln(f_c/f_g))^*$ for H/D IEs of methyl fluoride is of opposite sign and ~ 3 to 4 larger than that for typical hydrocarbons, $\sim +0.03$ or $+0.04$ per D as compared to typically -0.01 per D). The VCIE data are at higher T , but similar considerations apply. Because of the specific nature of the interaction, an LJ model calculation is inappropriate.

(b) *Ethane* $\text{C}_2\text{H}_6/\text{C}_2\text{D}_6$. There is reasonable agreement between $\ln(f_c/f_g)^*$, data and the LJ model, but this is dependent on setting the contribution of the internal rotation in the gas-dimer partition function ratio equal to its contribution to the gas-liquid ratio. (See Table 4).

(c) *Ethylene* $\text{C}_2\text{H}_4/\text{C}_2\text{D}_4/\text{C}_2\text{H}_2\text{D}_2$ (Table 4). Again, there is reasonable agreement between $\ln(f_c/f_g)^*$ and $\ln(f_p/f_g^2)$ data and the model calculations.

(d) *Neopentane* $\text{C}(\text{CH}_3)_4/\text{C}(\text{CH}_3)_3\text{CD}_3/\text{C}(\text{CH}_3)_2(\text{CD}_3)_2/\text{C}(\text{CH}_3)(\text{CD}_3)_3/\text{C}(\text{CD}_3)_4$. The VCIE data are not precise enough to warrant a two parameter fit. That $A_p < 0$ (Table 2) most likely indicates that the methyl torsional motions red shift on condensation to the liquid. For the gas-phase dimer, the reduced masses and moments of inertia are large and $(A_p/T^2) \ll (B_p/T)$; the bulk of the VCIE is due to the shift in internal frequencies. It is not useful to pursue the LJ description of the external mode contributions.

(e) *Ammonia* NH_3/ND_3 and *Methylamine* $\text{CH}_3\text{NH}_2/\text{CH}_3\text{ND}_2$. Large A terms result from H-bonding in the dimer or liquid states. The LJ formalism is not useful because dispersive contributions are overwhelmed by large directionally specific H-bonding contributions.

(f) *Methylamine* $\text{CH}_3\text{NH}_2/\text{CD}_3\text{NH}_2$. The sign of the A terms is negative, and this is unexpected. It most likely indicates a red shift for the torsional motion of the CH_3 group in dimer or condensed phase relative to the dilute gas due to H-bonding at the other end of the molecule. The LJ contribution is unimportant as compared to the consequences of the H-bonding.

(g) *Methylamine* $\text{CH}_3\text{NH}_2/\text{CD}_3\text{ND}_2$. To within experimental precision, the effects are those calculated assuming additivity ($\text{D5} = \text{D3} + \text{D2}$).

(h) *Water* $\text{H}_2\text{O}/\text{D}_2\text{O}$. Large A and B terms result from H-bonding in dimer or liquid. These effects cannot be properly treated using LJ analysis.

Conclusion

Isotope effects on the vapor phase second virial coefficient and on vapor pressure share a common origin. They are approximately proportional to one another, $\ln(f_p/f_g^2) = (-\text{VCIE}) = (0.4 \pm 0.2) \ln(f_c/f_g)^*$, provided the comparisons are made not too close to either crossover temperature. Both $\ln(f_p/f_g^2)$ and $\ln(f_c/f_g)^*$ depend on temperature in a complicated fashion; $\ln(f_c/f_g)^*$ or $\ln(f_p/f_g^2) = A/T^2 + B/T$. For many compounds, the A and B terms are of opposite sign but of commensurate magnitude, and in such cases $\ln(f_c/f_g)^*$ or $\ln(f_p/f_g^2)$ amounts to a small difference between much larger terms and may be either positive (normal) or negative (inverse). Ordinarily, the A contribution results from quantization of the overall motions of the molecule of interest (external modes) upon transfer from the gas phase to the condensed phase or interacting vapor pair and is positive. The formalism developed in this paper to compare $\ln(f_c/f_g)^*$, referring to VPIE, and $\ln(f_p/f_g^2)$, referring to $(-\text{VCIE})$, treats the (vapor monomer = n -coordinated liquid) and (vapor monomer = vapor pair) equilibria analogously and focuses attention on their common origin.

Acknowledgment. Research at The University of Tennessee was supported by the Ziegler Research Fund.

Appendix A: The Genesis of Eqs 6, 10, and 12. The A/B Equations

In 1963 Stern, Van Hook and Wolfsberg¹³ presented a formalism for the calculation of VPIE from input data that includes complete force fields (or frequency data) for the ideal gas and condensed phases, and that approach has been extended to the VCIE in the present paper, in which case the spectroscopic data (or the equivalent force constants and force constant shifts) refer to the ideal gas and gas phase dimer species. The formalism is usually presented in the harmonic approximation. Generalization to anharmonic force field appears possible, albeit complicated. In the gas, the partition functions for translation and rotation are evaluated classically, and no vibration-rotation interaction is assumed. The type of calculation we are doing is often referred to as a rigid-rotor-harmonic-oscillator calculation. The reduced partition function ratio in the gas for a nonlinear n -atom molecule is then

$$(s/s')f_g = (Q_{\text{QM}}/Q'_{\text{QM}})/(Q_{\text{CL}}/Q'_{\text{CL}}) = (Q_{\text{VIB,QM}}/Q'_{\text{VIB,QM}}) / (Q_{\text{VIB,CL}}/Q'_{\text{VIB,CL}}) = \prod_{i=1}^{3n-6} [u_i/u'_i] \{ \exp(-u_i/2) / (1 - \exp(-u_i)) \} / \{ \exp(u'_i/2) / (1 - \exp(-u'_i)) \} \quad (\text{A-1})$$

where $Q_{\text{VIB,QM}}$ is the quantum mechanical, and $Q'_{\text{VIB,CL}}$ is the classical vibrational partition function

$$Q_{\text{VIB,QM}} = \prod_{i=1}^{3n-6} \exp(-u_i/2) / (1 - \exp(-u_i))$$

$$Q_{\text{VIB,CL}} = \prod_{i=1}^{3n-6} (1/u_i) \quad (\text{A-2})$$

and $u_i = hc\nu_i/kT$, ν_i is the i th normal mode vibrational frequency in wavenumbers. At low rotational temperatures, a correction for nonclassical rotation may be necessary. In eq 1, s and s' are symmetry numbers, which have been dropped from eqs 3

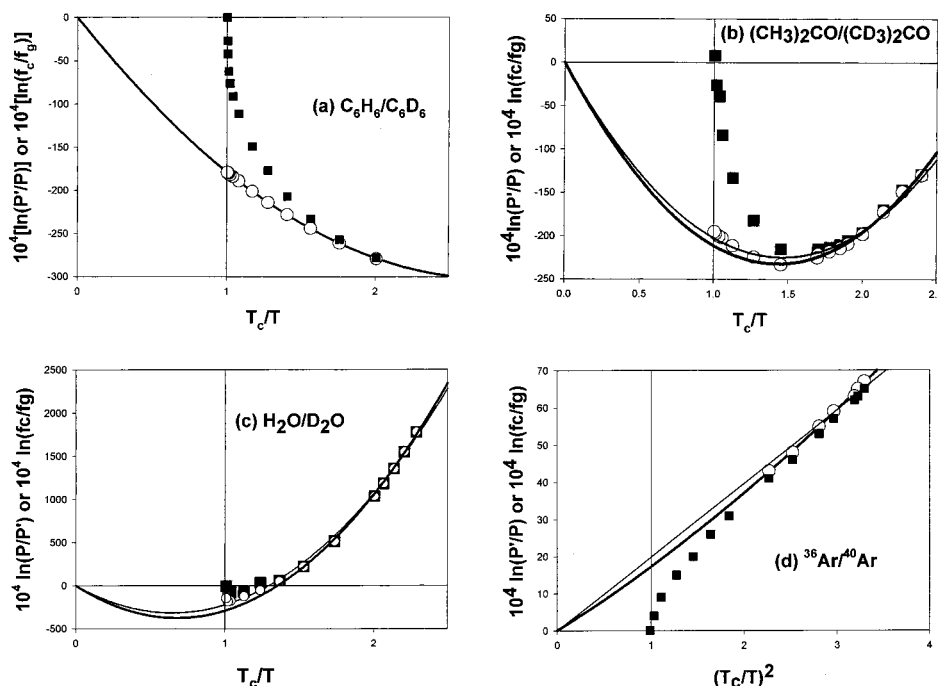


Figure 6. $\ln(P/P) = \text{VPIE}$ and $\ln(f_c/f_g)$ for some systems where measurements of vapor pressure and molar volume and virial coefficient corrections have been made over most of the range ($T_{\text{TRIPLE}} < T < T_{\text{CRITICAL}}$). In each case, the filled squares designate $\ln(f_c/f_g)$, the filled circles designate $\ln(P/P)$. (a) $\text{C}_6\text{H}_6/\text{C}_6\text{D}_6$ (ref 50). The heavy solid line is the least-squares fit to data extending across the entire temperature range, $\ln(P/P) = 39/T_r^2 - 218/T_r$. On the scale of the figure, it cannot be distinguished from the fit to the low temperature ($T/T_{\text{CRITICAL}} < \sim 0.7$) data only (b) $(\text{CH}_3)_2\text{CO}/(\text{CD}_3)_2\text{CO}$ (ref 50). The lighter line is the least-squares fit to data extending across the entire temperature range, $\ln(P/P) = 105/T_r^2 - 307/T_r$, the heavier line is the fit to the low temperature ($T/T_{\text{CRITICAL}} < 0.7$) data, $\ln(P/P) \sim \ln(f_c/f_g)^* = 113/T_r^2 - 324/T_r$. (c) $\text{H}_2\text{O}/\text{D}_2\text{O}$ (ref 50). The lighter line is the least-squares fit to data extending across the entire temperature range, $\ln(P/P) = 756/T_r^2 - 980/T_r$, the heavier line is the fit to the low temperature ($T/T_{\text{CRITICAL}} < 0.7$) data, $\ln(P/P) \sim \ln(f_c/f_g)^* = 819/T_r^2 - 1112/T_r$. (d) $^{36}\text{Ar}/^{40}\text{Ar}$ (refs 22, 61). The lighter line is the least-squares fit to the low temperature ($T/T_{\text{CRITICAL}} < 0.7$) data, $\ln(P/P) \sim \ln(f_c/f_g)^* = 19.8/T_r^2$, the heavier line is a two parameter fit to that same data $\ln(P/P) \sim \ln(f_c/f_g)^* = 15.9/T_r^2 + 1.3/T_r^4$.

through 10 for economy of notation since they do not impact present considerations.

In the condensed or vapor pair states, we choose a simplified model that assumes an average condensed phase molecule with $3n$ degrees of freedom, or interacting pair with $2*3n$ degrees of freedom. The $(3n - 6)_c$ or $2(3n - 6)_p$ internal vibrational modes are treated in strict analogy to the gas phase, and the remaining external degrees of freedom (6 for the condensed molecule, and 12 for the dimer, but 6 of those are null frequencies) are assumed to be subject to harmonic restoring forces. These assumptions yield

$$f_c = \prod_{i=1}^{3n} [u_i/u_i']_c \{ \exp(-u_i/2)/(1 - \exp(-u_i)) \} \{ \exp(-u_i'/2)/(1 - \exp(-u_i')) \}_c \quad (\text{A-3})$$

$$f_c/f_g = \prod_{\text{Ints}}^{3n-6} (L_c M_c) * \prod_{\text{Exts}}^6 (N_c) \quad (\text{A-4})$$

and

$$f_p = \prod_{i=1}^{2*3n-6} [u_i/u_i']_p \{ \exp(-u_i/2)/(1 - \exp(-u_i)) \} \{ \exp(-u_i'/2)/(1 - \exp(-u_i')) \}_p \quad (\text{A-5})$$

$$f_p/f_g^2 = \prod_{\text{Ints.}}^{2*3n-6} (L_d M_d) \prod_{\text{Exts.}}^{2*3n-6} (N_d) \quad (\text{A-6})$$

where $L_{c \text{ or } p} = [(u_i/u_i')_{c \text{ or } p} / (u_i/u_i')_g] \{ \exp((u_i' - u_i)_{c \text{ or } p}/2) / \exp((u_i' - u_i)_g) \}$

$- u_i)_g/2)$, $M = [(1 - \exp(-u_i)_{c \text{ or } p}) / (1 - \exp(-u_i)_{c \text{ or } p})] / [(1 - \exp(-u_i)_g) / (1 - \exp(-u_i)_g)]$, and $N = [u_i/u_i']_{c \text{ or } p} \{ \exp((u_i' - u_i)_{c \text{ or } p}/2) \} / [u_i/u_i']_{c \text{ or } p} \{ \exp((u_i' - u_i)_g/2) \} / [(1 - \exp(-u_i)_{c \text{ or } p}) / (1 - \exp(-u_i)_g)]$.

A common approximation makes use of the fact that very often the $3n$ normal modes per molecule fall neatly into two groups. The first group contains the high frequencies $u_i \gg 1$ and may be treated in the zero point energy (low temperature) approximation because excitation factors for these frequencies all approach unity. The second group contains only low frequencies and is treated in the high-temperature approximation. For the low-frequency group, one employs the expansion of $\ln(f)$ in even powers of u_i^{12}

$$\ln f_i = \sum_{j=1}^{\infty} (-1)^{j+1} B_{2j-1} (u_i^{2j} - u_i'^{2j}) / [(2j)(2j!)] \quad (u_i < 2\pi)$$

$$\ln f = \sum_{\text{low freqs}} \ln(f_i) \quad (\text{A-7})$$

The B 's are the Bernoulli numbers, $B_1 = 1/6$, $B_2 = 1/30$, etc. As is well-known, the logarithm of the harmonic oscillator partition function in the zero point (low-temperature, high-frequency) approximation reduces to $u/2$, so the contribution from the high-frequency group is of the form

$$\ln f_{\text{HIGH}} = \sum_{\text{High Frequencies}} (u_i' - u_i)/2 \quad (u_i \gg 1) \quad (\text{A-8})$$

With proper reorganization and labeling, and using just the first term of the expansion in eq 7, one obtains (recognizing that six of the external dimer modes are null frequencies)

$$\ln(f_p/f_g^2) = A_p/T^2 + B_p/T = (1/24)(hc/kT)^2 \left\{ \sum_{i=1}^5 [(v_i^2 - v_i^2)_{\text{Bend,Int. Rot}}] + (v_i^2 - v_i^2)_{\text{LJ}} \right\} + \frac{1}{2(3n-6)} (1/2)(hc/kT) \left(\sum [(v_i' - v_i)_p - (v_i' - v_i)_g] \right)_{\text{INT}} \quad (\text{A-9})$$

The analogous equation for $\ln(f_c/f_g)^*$ is obtained from eqs A-5 and A-6,

$$\ln(f_c/f_g)^* = A_c/T^2 + B_c/T = (1/24)(hc/kT)^2 \left\{ \sum_{i=1}^6 [(v_i^2 - v_i^2)_{\text{EXT.lattice modes}}]_c + \frac{1}{2(3n-6)} (1/2)(hc/kT) \left(\sum [(v_i' - v_i)_c - (v_i' - v_i)_g] \right)_{\text{INT}} \right\} \quad (\text{A-10})$$

Equations A-9 and A-10 are eqs 12a and 12b of the main text.

Appendix B: The Behavior at High Temperature

Kooner and Van Hook⁵⁰ have examined the behavior of eq 4 (slightly modified) as T and P increase toward the critical region.

$$\ln(f_c/f_g) = \ln(P'/P) - (P'V'_c - PV_c)/RT + (1/(RT)) \left[\int_0^{P'} \alpha' dP - \int_0^P \alpha dP \right] \quad (\text{B-1})$$

The third term on the right is the correction for vapor nonideality, which at lower pressures can be conveniently reexpressed using the virial expansion.

$$\left[\int_0^{P'} \alpha' dP - \int_0^P \alpha dP \right] / RT = (1/RT) \left[\int_0^{P'} (V - RT/P)' dP' - \int_0^P (V - RT/P) dP \right] \sim [(\mathcal{B}'_0 P' + (1/2) \mathcal{C}'_0 P'^2) - (\mathcal{B}_0 P + (1/2) \mathcal{C}_0 P^2)] / (RT) \quad (\text{B-2})$$

which is the form used in eq 4. At high pressure, however, the virial expansion is not useful; too many higher order terms are required, and close to the critical pressure the formalism is not useful at all. The authors⁵⁰ reported new data that extends to the immediate vicinity of the critical point for $\text{C}_6\text{H}_6/\text{C}_6\text{D}_6$, $\text{CH}_3\text{-CO}/\text{CD}_3\text{CO}$, and $\text{CH}_3\text{OH}/\text{CH}_3\text{OD}$, and examined literature data for CH_4/CD_4 and $\text{H}_2\text{O}/\text{D}_2\text{O}$. Figure 6, panels a, b, and c, illustrate their comparisons of $\ln(f_c/f_g)$ and $\ln(P'/P)$ for three of these pairs, and Figure 6d represents a similar comparison for $^{40}\text{Ar}/^{36}\text{Ar}$.^{21,22,27,61,62} In each case, within experimental precision $\ln(f_c/f_g)$ is small at $T_R = T/T_{\text{CRIT}} = 1$. The point of present interest is that least-squares fits of $\ln(P'/P)$ using the form of eq 6 (or, for Ar, an appropriate modification) accurately represent the data in each case, and for T low enough, say $T_R = T/T_{\text{CRIT}} < \sim 0.7$, $\ln(P'/P)$ and $\ln(f_c/f_g)$ coincide to sufficient precision. We note that to good approximation $\ln a = \text{LVFF}$ (liquid-vapor-fractionation-factor) = $\ln(f_c/f_g)$ over the entire liquid range ($T_{\text{TRIPLE}} < T < T_{\text{CRITICAL}}$).

While, as shown in Appendix A, eqs 6 and A-10 model $\ln(f_c/f_g)$ in the harmonic oscillator approximation to good precision, the agreement obviously fails as T_R increases. A better approach at high temperature employs the pseudo-harmonic approximation. This method assumes the frequency shifts, condensed to vapor phase, and their associated force constants and force constant shifts, are some simple function of the molar volumes and molar volume differences of equilibrating phases and therefore depend on temperature only indirectly (i.e., via the expansivity). In one such approach, a Gruneisen approximation

is written for each of the i isotope dependent frequencies or frequency shifts, $(d \ln \nu_{\text{liq}}/d \ln V_{\text{liq}})_i = \gamma_i$, where γ_i is a parameter. These methods have been thoroughly reviewed.^{14,17,58} In a more general formulation, Bigeleisen and co-workers reviewed the use of isotope effect studies to establish the mean square force in simple liquids and to calculate the mean force constants of the rare gases and the rectilinear law of mean force.^{61,62} This author and co-workers conclude that in the approximation where excess effects on mixing of isotopes are neglected liquid/vapor isotope fractionation factors, $\ln(\alpha)$, are expected to scale as $\ln(f_c/f_g)$, and this persists to the critical point.²¹ This is consequent to the proportional scaling of $\langle \nabla^2 U \rangle$ (and thus the A and B parameters as well) with orthobaric density.

The present interest, however, lies not in the high-temperature orthobaric approach to the critical pressure but in the properties of the low-temperature liquid. The approximation $\ln(P'/P) \sim \ln(f_c/f_g)^* = A/T^2 + B/T$ for $T_r < \sim 0.7$, with A and B calculated in the harmonic approximation using eq 10, makes use of the observations that the expansivity of the low temperature liquid is small and the vapor is nearly ideal. Over the temperature ranges specified in Table 2, typically ($\sim 0.5 < T_r < 0.67$), the liquid expands by $\sim 10\%$.⁶³ The use of temperature averaged A_c and B_c over that range is warranted for present purposes, and this conclusion is supported by the statistical quality of the $\ln(P'/P)^* = A_c/T^2 + B_c/T$ fits shown in Figures 2, 3, and 6, and reported in Table 2. At the temperatures of interest to us, $T_r < \sim 0.7$ pseudo-harmonic corrections, while important for the understanding of isotope effects on excess free energies of mixing, and for rationalizing certain fine points of interpretation of VPIEs, are small.^{14,17,18}

References and Notes

- (1) Van Hook, W. A.; Wolfsberg, M. Z. *Naturforsch.* **1994**, *49A*, 563.
- (2) Wolfsberg, M. *J. Chim. Phys.* **1963**, 15.
- (3) Grigor, A. F.; Steele, W. A. *J. Chem. Phys.* **1968**, *48*, 1033. Steele, W. A. *J. Chem. Phys.* **1969**, *50*, 562. Steele, W. A. *J. Chem. Phys.* **1961**, *34*, 802. Derberian, E. A.; Steele, W. A. *J. Chem. Phys.* **1971**, *55*, 5795.
- (4) Bigeleisen, J.; Wolfsberg, M. *J. Chem. Phys.* **1969**, *50*, 561.
- (5) Fang, A. Y.; Van Hook, W. A. *J. Chem. Phys.* **1968**, *60*, 3513.
- (6) Gainar, I.; Strein, K.; Schramm, B. *Ber. Bunsen-Ges. Phys. Chem.* **1972**, *76*, 1242.
- (7) Gainar, I.; Schafer, K.; Schmeisser, B.; Schramm, B.; Strein, K. *Ber. Bunsen-Ges. Phys. Chem.* **1973**, *77*, 372.
- (8) Gopel, W.; Dorfmueller, T. Z. *Phys. Chem.* **1972**, *82*, 54.
- (9) Singh, R. R.; Van Hook, W. A. *Macromolecules* **1987**, *20*, 1855.
- (10) Bates, F. S.; Keith, H. D.; McWhan, D. B. *Macromolecules* **1987**, *20*, 3065.
- (11) Hirschfelder, J. O.; Curtiss, C. F.; Bird, R. B. *Molecular Theory of Gases and Liquids*; Wiley: New York, 1954.
- (12) Bigeleisen, J. *J. Chem. Phys.* **1961**, *34*, 1485.
- (13) Stern, M. J.; Van Hook, W. A.; Wolfsberg, M. *J. Chem. Phys.* **1963**, *39*, 3179.
- (14) Jancso, G.; Van Hook, W. A. *Chem. Rev.* **1974**, *74*, 689.
- (15) Wolfsberg, M. *Annu. Rev. Phys. Chem.* **1969**, *20*, 449. Kleinman, L.; Wolfsberg, M. *J. Chem. Phys.* **1973**, *59*, 2043; **1974**, *60*, 4740.
- (16) Bigeleisen, J.; Mayer, M. G. *J. Chem. Phys.* **1947**, *15*, 261.
- (17) Jancso, G.; Rebelo, L. P.; Van Hook, W. A. *Chem. Rev.* **1993**, *93*, 2645.
- (18) Jancso, G.; Rebelo, L. P.; Van Hook, W. A. *Chem. Soc. Rev.* **1994**, 257.
- (19) Calado, J. C. G.; Nunes da Ponte, M.; Rebelo, L. P. N.; Staveley, L. A. K. *J. Phys. Chem.* **1989**, *93*, 3355.
- (20) Calado, J. C. G.; Lopes, J. N. C.; Nunes da Ponte, M.; Rebelo, L. P. N. *J. Chem. Phys.* **1997**, *106*, 8792.
- (21) Popowicz, A. M.; Lu, T. H.; Bigeleisen, J. Z. *Naturforsch.* **1991**, *46A*, 60.
- (22) Calado, J. C. G.; Dias, F. A.; Lopes, J. N. C.; Rebelo, L. P. N. *J. Phys. Chem.* **2000**, *104*, 8735.
- (23) Lee, M.; Fuks, S.; Bigeleisen, J. *J. Chem. Phys.* **1970**, *53*, 4066.
- (24) Munster, A. *Statistical Thermodynamics*, Vol. 1, Springer: Berlin, 1969.
- (25) Rice, O. K. *Statistical Mechanics, Thermodynamics, and Kinetics*; W. H. Freeman: San Francisco, 1967: Chapter 8.

- (26) De Boer, J.; Michels, A. *Physica* **1938**, *5*, 945.
- (27) Phillips, J. T.; Linderstrom-Lang, C. U.; Bigeleisen, J. *J. Chem. Phys.* **1972**, *56*, 5053.
- (28) Moelwyn-Hughes, E. A. *Physical Chemistry*; Pergamon: New York, 1957; Chapter VII.
- (29) Lennard-Jones, J. E.; Ingham, A. E. *Proc. R. Soc.* **1925**, *A107*, 636.
- (30) Moelwyn-Hughes²⁸ writes the effective intermolecular (pair) potential for the gas-gas dimer as $u_d(R_{12}) = C_n R_{12}^{-n} - C_m R_{12}^{-m}$, and of the condensed phase (N atom [molecule] lattice) as $u_c(R_{12}) = c(C_n s_n R_{12}^{-n} - C_m s_m R_{12}^{-m})$. Here c is the number of nearest neighbors and s_n and s_m are constants obtained from lattice sums and are tabulated for various lattices and "smeared" liquid structures.²⁸ The ratio of equilibrium intermolecular distances is given by $(R_{12,d}/R_{12,c})^{n-m} = s_m/s_n$, the ratio of well depths $\epsilon_{\text{COND}}/\epsilon_{\text{DIMER}} = c(s_n^{n/(n-m)}/s_m^{m/(n-m)})$. For the condensed phase, the three Cartesian force constants (that is, the curvatures (second derivatives) of the pair potential evaluated at the minimum) are calculated on the assumption of spherical symmetry around each lattice position, so the three values κ_{xx} , κ_{yy} , and κ_{zz} are equal. These force constants are referred to as κ_c which may be compared with the force constant κ_p of the gas-gas pair (derived by taking the second derivative of $u_p(R_{12})$ above). MH finds $(\kappa_p/\kappa_c) = 3(s_n/s_m)^{2.33}/c s_n$ for $n = 12$, $m = 6$. For the smeared FCC structure with $c = 12$ this yields $(\kappa_p/\kappa_c) = 0.17$. One can calculate the harmonic frequencies of the N -atomic lattice by diagonalizing the Cartesian force constant matrix corresponding to mass weighted Cartesian coordinates; the diagonal elements of this matrix contain three elements for each atom, each of which is equal to κ_c/m . It is well-known that the sum of the squares of the $3N$ lattice frequencies is $[(2\pi)^{-2}(3N\kappa_c)/m]$; each atom contributes effectively $[(2\pi)^{-2}(3\kappa_c)/m]$. MH designates $(1/2\pi)(\kappa_c/m)^{1/2}$ as the lattice frequency ν_c , where m is the mass corresponding to the lattice position. He reasons this to be correct on the assumption that each atom vibrates against the total lattice. This is an approximation since in truth there is a band of frequencies. This is further discussed in the following ref 31. MH then calculates (for the smeared FCC structure with $c = 12$) $(\nu_p/\nu_c)^2 \sim 0.33$ using $\nu = (\kappa/\mu)^{1/2}/(2\pi)$ and $\mu_c/\mu_p \sim 2$. For the BCC crystal ($c = 8$), one finds similarly $(\kappa_d/\kappa_c) = 0.16$ and $(\nu_p/\nu_c)^2 \sim 0.33$, while for the rock salt lattice ($c = 6$) $(\kappa_p/\kappa_c) = 0.24$ and $(\nu_p/\nu_c)^2 \sim 0.48$. The effect of condensation is to bring the molecules some 3 to 5% closer, to increase the vibrational frequency for the external degree of freedom by roughly 60%, and to provide an average potential energy greater than the near pairs value, $(c/2)^* \epsilon_{\text{DIMER}}$ by 40 to 60% or more.
- (31) We have indicated above³⁰ how Moelwyn-Hughes²⁸ evaluates the lattice force constant κ_c and approximate lattice frequency ν_c . Our main use of ν_p is the evaluation of A_c in eq 12b. It should be noted that eq 12b requires only the contribution of each lattice point to the sum of the squares of the harmonic vibrational frequencies. From the above,³⁰ we know that this sum is given exactly by $3\nu_c^2$.
- (32) Bigeleisen, J.; Cragg, C. B.; Jeevanandam, M. *J. Chem. Phys.* **1967**, *47*, 4335.
- (33) Lide, D. R., Ed. *Handbook Chemistry and Physics*, 71st ed.; CRC Press, Boca Raton, FL, 1991.
- (34) Van Hook, W. A. *J. Phys. Chem.* **1968**, *72*, 1234.
- (35) Keenan, J. H.; Keyes, F. G.; Hill, P. G.; Moore, J. G. *Steam Tables; Thermodynamic Properties of Water*; John Wiley and Sons: New York, 1969.
- (36) For monatomic species one has $\ln(f_p/f_g^2)/\ln(f_c/f_g^2)^* = A_p/A_c = (n_p/\nu_c)(\nu_p^2/\nu_c^2) \sim (1/3)(0.4)$ since there is 1 dimer frequency but 3 condensed phase lattice modes per molecule. For polyatomic species $A_p/A_c = (n_{p,LJ}\nu_{p,LJ}^2 + n_{p,rot}\nu_{p,rot}^2)/(n_{c,LJ}\nu_{c,LJ}^2 + n_{c,rot}\nu_{c,rot}^2) \sim (\nu_{p,LJ}^2 + 5\nu_{p,rot}^2)/(6\nu_{c,LJ}^2 + 6\nu_{c,rot}^2) \sim (1/2)(0.33)$ if $\nu_{p,LJ}^2 = \nu_{p,rot}^2$ and $\nu_{c,LJ}^2 = \nu_{c,rot}^2$. If, as may be likely (vide infra), $\nu_{p,rot}^2 > \nu_{p,LJ}^2$, A_p/A_c will be larger. For diatomics and polyatomics
- $B_p/B_c = (\sum \delta\Delta\nu)_p/(\sum \delta\Delta\nu)_c \sim (\delta\kappa_p/\delta\kappa_c)_{\text{INT}}$ assuming (as is unlikely) that the fractional shift in internal force constants on dimer formation scales proportionally to that on condensation for each of the $2(3n - 6)$ internal modes. As previously, Δ denotes an isotopic difference, δ a phase difference. If, further, $(\delta\kappa_p/\delta\kappa_c)_{\text{INT}} \sim (\delta\kappa_p/\delta\kappa_c)_{\text{EXT}}$, $LJ = (\kappa_p/\kappa_c)_{\text{EXT}}$, LJ , then $B_p/B_c \sim 0.2$, but this estimate is crude.
- (37) Dymond, J. H.; Smith, E. B. *The Virial Coefficients of Pure Gases and Mixtures. A Critical Compilation*; The Clarendon Press: Oxford, 1980.
- (38) Rebelo, L. P. N., manuscript in preparation.
- (39) Oi, T.; Shulman, J.; Popowicz, A.; Ishida, T. *J. Phys. Chem.* **1983**, *87*, 3153.
- (40) Van Hook, W. A. *J. Chem. Phys.* **1966**, *44*, 234.
- (41) Ishida, T.; Bigeleisen, J. *J. Chem. Phys.* **1968**, *49*, 5498.
- (42) Gopel, W.; Dorfmueller, T. *Z. Phys. Chem. Frankfurt* **1972**, *82*, 58.
- (43) Hopfner, A.; Parekh, N.; Horner, Ch.; Abdel-Hamid, A. *Ber. Buns. Phys. Chem.* **1975**, *79*, 217.
- (44) Wolff, H.; Hopfner, A. *Ber. Buns. Phys. Chem.* **1969**, *73*, 480.
- (45) Wolff, H.; Hopfner, A. *Ber. Buns. Phys. Chem.* **1965**, *69*, 710.
- (46) Henderson, C.; Lewis, D. G.; Prichard, P. C.; Staveley, L. A. K.; Fonseca, I. M. A.; Lobo, L. Q. *J. Chem. Thermodynamics* **1986**, *18*, 1077.
- (47) Schramm, B.; Leuchs, U. *Ber. Buns. Phys. Chem.* **1979**, *83*, 847.
- (48) Pupezin, J.; Jakli, G.; Jancso, G.; Van Hook, W. A. *J. Phys. Chem.* **1972**, *76*, 743.
- (49) Kell, G. S.; McLaurin, G. E.; Whalley, E. *J. Chem. Phys.* **1968**, *49*, 2839. Kell, G. S.; McLaurin, G. E.; Whalley, E. *Proc. R. Soc.* **A425**, *49*, 1989.
- (50) Kooner, Z. S.; Van Hook, W. A. *J. Phys. Chem.* **1988**, *92*, 6414.
- (51) Even so, the information that VCIE = 0 for HCl/DCl is important. It reinforces the conclusion that VCIE and VPIE scale one to another. Note that this pair exhibits a crossover in vapor pressure (VPIE = 0) around 223 K and another in molar volume (~ 192 K).⁴⁶ The effects have been interpreted in the framework of the statistical theory of isotope effects.^{52,53}
- (52) Lopes, J. N. C.; Calado, J. C. G.; Jancso, G. *J. Phys. Condens. Matter* **1992**, *4*, 6691.
- (53) Lewis, D. G.; Staveley, L. A. K.; Lobo, L. Q. *J. Phys. Chem.* **1986**, *90*, 5456.
- (54) SigmaPlot5.0, Help menu. Taylor, John R. *An Introduction to Error Analysis*; Oxford University Press: Oxford, 1982.
- (55) Aziz, R. A.; Chen, H. H. *J. Chem. Phys.* **1977**, *67*, 5719.
- (56) Lee, M. Y.; Bigeleisen, J. *J. Chem. Phys.* **1977**, *67*, 5634.
- (57) Fischer, J.; Lusting, R.; Breitenfelder-Manske, H.; Lemming, W. *Mol. Phys.* **1984**, *52*, 485.
- (58) The long established use of temperature-dependent lattice frequencies in the theoretical interpretation of VPIE data been reviewed by Van Hook and co-workers.^{14,17} Typically, a Gruneisen model is employed to couple the frequency shift to the volume change due to thermal expansion, $-\ln\nu_{\text{LATTICE}}/dT \sim \gamma d\ln V/dT \sim \gamma\alpha$. Here γ is the Gruneisen constant, sometimes available from thermodynamic analysis, sometimes from spectroscopic measurements, and α is the coefficient of thermal expansion.⁵⁹
- (59) Lopes, J. N. C.; Rebelo, L. P. N.; Jancso, G. *J. Mol. Liq.* **1992**, *54*, 115.
- (60) Van Hook, W. A.; Rebelo, L. P. N.; Wolfsberg, M., manuscript in preparation.
- (61) Bigeleisen, J.; Lee, M. W.; Mandel, F. *Acc. Chem. Res.* **1975**, *8*, 179.
- (62) Lee, M. W.; Bigeleisen, J. *J. Chem. Phys.* **1977**, *67*, 5634.
- (63) National Institute of Standards and Technology; Chemistry Web Data Bank (<http://webbook.nist.gov/cgi>). Landolt-Bornstein, Tabellen, Mechanische und Thermische Zustandsgr.; Springer-Verlag: Berlin, 1971.
- (64) Thomaes, G.; van Steenwinkel, R. *Mol. Phys.* **1962**, *5*, 307.